World Journal of Gastroenterology

Submit a Manuscript: https://www.f6publishing.com

World J Gastroenterol 2024 March 7; 30(9): 1189-1212

DOI: 10.3748/wjg.v30.i9.1189

ISSN 1007-9327 (print) ISSN 2219-2840 (online)

ORIGINAL ARTICLE

Basic Study

Uridine diphosphate glucuronosyltransferase 1A1 prevents the progression of liver injury

Jin-Lian Jiang, Yi-Yang Zhou, Wei-Wei Zhong, Lin-Yan Luo, Si-Ying Liu, Xiao-Yu Xie, Mao-Yuan Mu, Zhi-Gang Jiang, Yuan Xue, Jian Zhang, Yi-Huai He

Specialty type: Gastroenterology and hepatology

Provenance and peer review: Invited article; Externally peer reviewed.

Peer-review model: Single blind

Peer-review report's scientific quality classification

Grade A (Excellent): 0
Grade B (Very good): B, B
Grade C (Good): 0
Grade D (Fair): 0
Grade E (Poor): 0

P-Reviewer: Dabbous H, Egypt; Li WD, China

Received: September 28, 2023
Peer-review started: September 28, 2023
First decision: December 6, 2023
Revised: January 2, 2024
Accepted: January 29, 2024
Article in press: January 29, 2024
Published online: March 7, 2024

Jin-Lian Jiang, Yi-Yang Zhou, Si-Ying Liu, Yi-Huai He, Department of Infectious Diseases, Affiliated Hospital of Zunyi Medical University, Zunyi 563000, Guizhou Province, China

Wei-Wei Zhong, Department of Infectious Diseases, Jingmen Central Hospital, Jingmen 448000, Hubei Province, China

Lin-Yan Luo, Department of Respiratory Medicine, Anshun People's Hospital, Anshun 561099, Guizhou Province, China

Xiao-Yu Xie, Department of General Practice, Affiliated Hospital of Zunyi Medical University, Zunyi 563000, Guizhou Province, China

Mao-Yuan Mu, Department of Intervention Radiology, Affiliated Hospital of Zunyi Medical University, Zunyi 563000, Guizhou Province, China

Zhi-Gang Jiang, School of Public Health, Zunyi Medical University, Zunyi 563099, Guizhou Province, China

Yuan Xue, Department of Liver Diseases, Third People's Hospital of Changzhou, Changzhou 213000, Jiangsu Province, China

Jian Zhang, Department of Digestion, Dafang County People's Hospital, Bijie 551600, Guizhou Province, China

Corresponding author: Yi-Huai He, MD, Director, Department of Infectious Diseases, Affiliated Hospital of Zunyi Medical University, No. 149 Dalian Road, Zunyi 563000, Guizhou Province, China. 993565989@qq.com

Abstract

BACKGROUND

Uridine diphosphate glucuronosyltransferase 1A1 (UGT1A1) plays a crucial role in metabolizing and detoxifying endogenous and exogenous substances. However, its contribution to the progression of liver damage remains unclear.

AIM

To determine the role and mechanism of UGT1A1 in liver damage progression.

METHODS

We investigated the relationship between UGT1A1 expression and liver injury through clinical research. Additionally, the impact and mechanism of UGT1A1 on the progression of liver injury was analyzed through a mouse model study.

RESULTS

Patients with *UGT1A1* gene mutations showed varying degrees of liver damage, while patients with acute-on-chronic liver failure (ACLF) exhibited relatively reduced levels of UGT1A1 protein in the liver as compared to patients with chronic hepatitis. This suggests that low UGT1A1 levels may be associated with the progression of liver damage. In mouse models of liver injury induced by carbon tetrachloride (CCl_4) and concanavalin A (ConA), the hepatic levels of UGT1A1 protein were found to be increased. In mice with lipopolysaccharide or liver steatosis-mediated liver-injury progression, the hepatic protein levels of UGT1A1 were decreased, which is consistent with the observations in patients with ACLF. *UGT1A1* knockout exacerbated CCl_4- and ConA-induced liver injury, hepatocyte apoptosis and necroptosis in mice, intensified hepatocyte endoplasmic reticulum (ER) stress and oxidative stress, and disrupted lipid metabolism.

CONCLUSION

UGT1A1 is upregulated as a compensatory response during liver injury, and interference with this upregulation process may worsen liver injury. UGT1A1 reduces ER stress, oxidative stress, and lipid metabolism disorder, thereby mitigating hepatocyte apoptosis and necroptosis.

Key Words: Uridine diphosphate glucuronosyltransferase 1A1; Liver injury progression; Endoplasmic reticulum stress; Oxidative stress; Lipid metabolism disorders

Core Tip: The role and mechanism of hepatic uridine diphosphate glucuronosyltransferase 1A1 (UGT1A1) in the progression of liver injury are still not fully understood. This study found that inhibiting compensatory upregulation of UGT1A1 promotes the progression of liver injury. The mechanism may be related to low levels of UGT1A1 exacerbating endoplasmic reticulum stress and oxidative stress, and disrupting lipid metabolism, thereby exacerbating hepatocyte apoptosis and necroptosis.

Citation: Jiang JL, Zhou YY, Zhong WW, Luo LY, Liu SY, Xie XY, Mu MY, Jiang ZG, Xue Y, Zhang J, He YH. Uridine diphosphate glucuronosyltransferase 1A1 prevents the progression of liver injury. *World J Gastroenterol* 2024; 30(9): 1189-1212
URL: https://www.wjgnet.com/1007-9327/full/v30/i9/1189.htm
DOI: https://dx.doi.org/10.3748/wjg.v30.i9.1189

INTRODUCTION

Uridine diphosphate glucuronosyltransferase 1A1 (UGT1A1) is a member of the phase II metabolic enzyme family; it is involved in the metabolism and detoxification of both endogenous and exogenous substances[1]. UGT1A1 can metabolize bilirubin and 7-ethyl-10-hydroxycamptothecin, which are well-known endogenous and exogenous substrates, respectively[2]. Bilirubin is produced from the breakdown of hemoglobin, and is primarily metabolized in the liver[3]. *UGT1A1* mutation can cause bilirubin metabolism disorders and accumulation. Current research indicates that *UGT1A1* mutation is a benign condition with no significant pathological response, and will not lead to hepatocyte death or chronic liver disease[4]. Moderate levels of bilirubin are effective physiological antioxidants[5], and may reduce oxidative stress, alleviate inflammation, prevent fibrosis, and ultimately affect the development of non-alcoholic fatty liver disease[6,7]. Furthermore, elevated levels of bilirubin can inhibit lipid oxidation and delay the development of atherosclerosis, thereby helping to prevent and counteract cardiovascular diseases such as coronary heart disease[8]. These findings suggest that the elevation of bilirubin, which has antioxidant effects, in individuals with *UGT1A1* mutation is beneficial to the human body.

However, high-frequency mutations in the *UGT1A1* gene can lead to hereditary hyperbilirubinemia[9], while a complete loss of *UGT1A1* function may be fatal, as *UGT1A1* knockout (KO) mice can survive for only approximately 20 d. Metabolic disorders associated with high bilirubin concentrations can cause neurotoxicity, resulting in irreversible damage to the brain and nervous system[10]. Animal experiments have shown that the intravenous infusion of bilirubin leads to hepatocellular cytoplasmic vacuolation and canalicular bile stasis[11], and high concentrations of accumulated bilirubin can cause liver toxicity[12]. Impaired UGT1A1 function increases the workload of the liver and can exacerbate liver damage caused by long-term bilirubin metabolism disorders[13]. In addition to metabolizing endogenous bilirubin, UGT1A1 participates in the metabolism of various exogenous drugs and harmful substances, thereby serving a detoxification role[14]. Decreased UGT1A1 activity in the body can cause drug metabolism disorders and drug accumulation,

which increases the drug exposure time and renders patients susceptible to drug-induced liver damage[15]. *UGT1A1* gene polymorphism and its gene product levels can serve as biomarkers for drug-induced liver injury[4]. Patients with Gilbert syndrome (GS) may be more susceptible to drug-induced liver injury after taking certain medications or undergoing biological therapies[16]. Research has shown that UGT1A1 is the major pathway for the glucuronidation of acetaminophen in the liver, and patients with low UGT1A1 enzyme activity are at risk for developing acute liver failure after the oral administration of acetaminophen[17]. First-line anti-tuberculosis drugs are commonly associated with hepatotoxicity, and *UGT1A1* gene mutation increases the risk of drug-induced liver disease from anti-tuberculosis drugs [18]. Tyrosine kinase inhibitors (TKIs) are substrates of UGT1A1 and compete with bilirubin for binding to UGT1A1. Pazopanib is a TKI that is used to treat advanced renal cell carcinoma. Studies have shown that in the presence of *UGT1A1* gene mutation, treatment with pazopanib for metastatic renal cell carcinoma increases the likelihood of hepatotoxicity, which can lead to the temporary or permanent discontinuation of the drug[19]. Other studies have confirmed that hyperbilirubinemia is observed in GS patients who receive TKI therapy, which increases the risk of liver damage and is closely related to low UGT1A1 activity[20]. We have previously reported the case of a patient with a *UGT1A1* mutation who developed significant bilirubin metabolism disorders and liver injury[21]. Therefore, the specific role of UGT1A1 dysfunction or low UGT1A1 levels in the progression of liver disease is yet to be elucidated.

The progression of liver disease is usually associated with persistent exposure to hepatotoxic factors, and in certain cases, it can manifest as a severe acute exacerbation (SAE) of liver disease[22]. SAE of liver disease is defined as the rapid deterioration of liver function within a short period of time, leading to the development of liver failure or decompensated cirrhosis against a background of pre-existing liver disease[23,24]. SAEs of liver disease usually involve 2 aspects: Sustained and relatively stable liver damage caused by various etiologies (such as hepatitis B virus infection and metabolic abnormalities), in conjunction with other factors that trigger acute liver damage, leading to the rapid deterioration of liver function.

Endotoxemia is commonly involved in the progression of liver diseases. Lipopolysaccharide (LPS), a primary component of endotoxins, can trigger cellular inflammatory responses and ultimately lead to liver-cell damage[25]; LPS can also directly damage hepatocytes[26]. Nevertheless, it is uncommon for LPS alone to cause significant liver injury [27]. LPS is often used as a trigger to exacerbate liver injury. Fatty liver is usually a disease that progresses slowly, but the presence of fatty degeneration in the liver increases the sensitivity of liver cells to injury; thus, fatty liver is a risk factor for the progression of liver damage[28]. It is unclear whether UGT1A1 is involved in the LPS- or liver steatosis-mediated exacerbation of liver injury.

Various pathogenic factors can damage the liver, leading to the programmed cell death of liver cells. Continued programmed cell death of the liver cells, which includes apoptosis and necroptosis, drives the progression of liver disease [29]. Apoptosis and necroptosis of liver cells are interconnected; each can influence and even transform into the other during the occurrence and development of various liver diseases. Caspase-3 is an essential executor in apoptosis, and its activation is regarded as a biomarker of cell apoptosis[30]. Necroptosis is a form of cell death that resembles necrosis in terms of morphological changes and shares similar regulatory mechanisms with apoptosis. Necroptosis is regulated by inflammatory signals, and is characterized by activation through the phosphorylation of the mixed lineage kinase domain-like pseudokinase (MLKL) region[31]. Endoplasmic reticulum (ER) stress and oxidative stress are defense responses that occur before hepatocyte apoptosis and programmed necrosis[32].

To clarify the relationship between UGT1A1 and the progression of liver damage, we analyzed the expression levels of UGT1A1 in patients with liver damage. In addition, we used a mouse model of liver damage to investigate the role and mechanism of UGT1A1 in the progression of liver damage at the systemic, cellular, and subcellular levels.

MATERIALS AND METHODS

Clinical research

The clinical data of patients with *UGT1A1* gene mutation detected by genetic testing for hereditary diseases were collected through our hospital's electronic medical record system. The relationship between *UGT1A1* gene mutation and liver damage was analyzed through liver-function tests, imaging studies, and pathological examinations.

In addition, liver tissue samples were obtained from patients with chronic hepatitis and those undergoing liver transplantation for acute-on-chronic liver failure (ACLF). These samples were subjected to proteomics analysis to evaluate variations in the expression levels of UGT1A1 protein in the liver. This clinical study was approved by the medical ethics committee of our hospital [approval numbers: ZYFYLS(2018)28 and ZYLS(2022)1-059], and informed consent was obtained from the patients prior to the collection of liver tissue samples.

Animal experiments

All animal studies were approved by the Animal Laboratory Studies Ethics Review Committee of Zunyi Medical University (ZMU21-2107-003 and ZMU11-2203-314). Healthy and clean male BALB/c mice (weight, 23.63 g ± 2.24 g) were purchased from the Animal Center of Zunyi Medical University [SYXK (Qian) 2021-0004, Guizhou, China]. The mice were kept in a pathogen-free facility at a controlled temperature of 20 °C-24 °C. They had unlimited access to food and water, and were maintained on a 12-h light/dark cycle. Once the mice had acclimated to their new environment, they were randomly assigned to different experimental groups by using a random number table. At least 12 mice per group were used for all studies, unless noted otherwise.

Induction of liver injury in mice

Carbon tetrachloride-induced liver injury: Carbon tetrachloride (CCl_4) is a widely known hepatotoxic substance that is frequently utilized as an agent to induce acute and chronic chemical liver injury[33]. BALB/c mice were randomly divided into 5 groups (of 12 mice each). The 0 h (control) group did not receive any treatment, while the 12 h, 24 h, 48 h, and 72 h groups received an intramuscular injection of a CCl_4 solution (Shanghai Macklin Biochemical Technology Co. Ltd., Shanghai, China) at a dose of 1.0 mL/kg. The mice were deprived of food and water for 6 h before the injection. Anesthesia was induced at 12 h, 24 h, 48 h, and 72 h following the CCl_4 injection, and orbital blood and liver tissue samples were collected from all the mice in all 5 groups.

Concanavalin A-induced liver injury: Concanavalin A (ConA) a lectin derived from jack bean, is frequently used to induce acute immune-mediated liver injury in mice[34]. BALB/c mice were randomly divided into 4 groups (of 12 mice each): The 12 h, 24 h, and 48 h groups, in which mice were intravenously injected with a 20 mg/kg dose of a ConA (Solarbio, Beijing, China) solution, and the 0 h (control) group, in which mice were intraperitoneally injected with an equal dose of normal saline. The mice were deprived of food and water for 6 h before the injections. The ConA solution was prepared by mixing ConA in a normal saline solution; the prepared solution was stored at 4 °C-8 °C until use. Anesthesia was induced at 0, 12 h, 24 h, and 48 h following the ConA/normal saline injections, and orbital blood and liver tissue samples were collected from all the mice.

LPS and CCl_4-induced SAE of liver injury: Mouse models of SAE of liver injury are usually established using long-term or chronic CCl_4 injections to induce chronic liver injury[35], followed by treatment with LPS or acetaminophen, or infection with *Klebsiella pneumoniae* to induce acute exacerbation of the liver injury[36,37]. In this study, BALB/c mice were randomly divided into 2 groups: The CCl_4 + LPS and the CCl_4 groups. In the CCl_4 + LPS group, mice were subcutaneously injected with 1.0 mL/kg of a CCl_4 solution, twice per week, for a duration of 8 wk. Additionally, they were intraperitoneally injected with 0.5 mg/kg LPS during the final CCl_4 injection. In the CCl_4 group, mice were administered only the CCl_4 solution, according to the same regimen as above. In both groups, the mice were deprived of food and water for 6 h before each injection. Anesthesia was induced at 24 h after the final injection, and orbital blood and liver tissue samples were collected from the mice.

Hepatosteatosis worsened liver injury caused by CCl_4: BALB/c mice were randomly divided into 4 groups. The control group received a normal diet for 8 wk. The high-fat diet (HFD; XTHF60; Jiangsu Xietong Pharmaceutical Bio-engineering Co. Ltd., Jiangsu Province, China) group received a diet consisting of 20% protein, 20% carbohydrates, and 60% fat for 8 wk. The CCl_4 group received a normal diet for 8 wk along with subcutaneous injections of a CCl_4 solution (1.0 mL/kg, twice weekly for 8 wk). The CCl_4 + HFD group received both the HFD and subcutaneous CCl_4 injections as above. Anesthesia was induced at 24 h after the final injection, and orbital blood and liver tissue samples were collected from the mice.

Ugt1a1 KO in vivo

BALB/c mice were randomly divided into 3 groups: The normal control group (untreated), the control group [control single guide ribonucleic acid (sgRNA)], and the Ugt1a1 sgRNA group (*Ugt1a1* sgRNA1, *Ugt1a1* sgRNA2, and *Ugt1a1* sgRNA3). In the control group and *Ugt1a1* sgRNA group, the mice were administered recombinant adenovirus (GeneChem, Beijing, China) containing control sgRNA and *Ugt1a1* sgRNA, respectively, *via* tail vein injections (5×10^{10}-1×10^{11} viral gene copies/mouse). The sequences of the sgRNAs used are shown in Table 1. At 6 wk after transfection, the protein levels of UGT1A1 were detected using western blot analysis, and the results were used to screen for the specific *Ugt1a1* sgRNA that knocked out the *Ugt1a1* gene.

To explore the effect of UGT1A1 on liver injury, we conducted research on animal models of acute liver injury induced by CCl_4 and ConA as well as on animal models of chronic liver injury induced by CCl_4. In the case of the acute CCl_4-induced liver injury model, a total of 48 mice were divided into 4 groups based on different sgRNAs: The control group (control sgRNA), *Ugt1a1* KO group (*Ugt1a1*-targeting sgRNA), CCl_4 group (control sgRNA + CCl_4), and *Ugt1a1*-KO + CCl_4 group (*Ugt1a1*-targeting sgRNA + CCl_4). In the case of the chronic CCl_4-induced liver injury model, a total of 24 mice were divided into 2 groups based on different sgRNAs: CCl_4 group (control sgRNA + CCl_4) and *Ugt1a1*-KO + CCl_4 group (*Ugt1a1*-targeting sgRNA + CCl_4). In the case of acute ConA-induced liver injury model, a total of 24 mice were divided into 2 groups based on different sgRNAs: ConA group (control sgRNA + ConA) and *Ugt1a1*-KO + ConA group (*Ugt1a1*-targeting sgRNA + ConA). Preliminary experiments revealed that the expression of ER stress- and oxidative stress-related proteins was most significant at the 24-h mark. Therefore, in the acute liver injury model, we selected 24 h after intramuscular CCl_4 injection (1.0 mL/kg) or intravenous ConA injection (20 mg/kg) as the observation point. In the chronic liver injury model, mice were subcutaneously injected with CCl_4 solution (1.0 mL/kg) twice weekly for 8 wk. The observation point was 24 h after the final injection. Anesthesia was induced at the appropriate observation time points in the acute and chronic liver injury models, and orbital blood and liver tissue samples were collected from all the mice.

Serum alanine transaminase, total bilirubin, and indirect bilirubin levels

Blood samples were collected from anesthetized mice, and the serum levels of alanine transaminase (ALT), total bilirubin (TBil), and indirect bilirubin (IBiL) were measured using a Beckman Coulter autoanalyzer (AU5800, Beckman Coulter, United States) in accordance with a standard protocol[38]. Specifically, the serum levels of ALT were quantified using the rate method, and the TBil and IBiL levels were analyzed using the diazo method.

Histopathological analysis

Liver tissues were fixed in 4% paraformaldehyde (Solarbio, Beijing, China) and then dehydrated, made transparent, embedded in paraffin, and sliced at 5-μm intervals. The paraffin sections were deparaffinized, dehydrated in gradient alcohol, washed with phosphate-buffered saline for 5 min, and stained with hematoxylin and eosin. For Masson trichrome staining, paraffin-embedded sections were deparaffinized with xylene, dehydrated in gradient alcohol, stained with the Masson staining solution supplemented with 5% phosphotungstic acid (Servicebio, Wuhan, Hubei Province, China), and then soaked in aniline solution. The stained sections were gradually dehydrated, cleaned with ethanol, and cleared with xylene. After the completion of the staining procedure, the sections were imaged using a Pannoramic Slicer (3D HISTECH CaseViewer, Pannoramic SCAN, Budapest, Hungary). The images were analyzed using CaseViewer *v* 2.4 software at various magnifications (1 × to 1000 ×, Budapest, Hungary). For the analysis of necrotic tissue, the target area was examined under 100 × magnification. Image-Pro Plus 6.0 software was used to measure the total area and the area of necrotic tissue, and the percentage of necrotic tissue was calculated as follows: Necrotic tissue percentage = necrotic tissue area/total tissue area × 100.

Apoptosis assay

Hepatocyte apoptosis in the liver tissue sections was detected using a commercially available terminal deoxynucleotidyl transferase-mediated deoxyuridine triphosphate-nick end labelling (TUNEL) assay kit (Roche, 11684817910), according to the manufacturer's instructions. Six areas were randomly selected on each slide to calculate the apoptotic index, which was determined as follows: Apoptotic index = number of positive cells/total number of cells × 100%.

Western blot analysis

Western blot analysis was conducted according to standard procedures by using lysates of tissue samples from the right hepatic lobes of the mice, as described previously[39]. In brief, the tissues were solubilized in lysis buffer containing phosphatase inhibitor (R0010, Solarbio, China). For determining the protein concentration, 40 μg of each sample was separated using sodium dodecyl sulfate polyacrylamide gel electrophoresis, and transferred to polyvinylidene fluoride membranes (Millipore, United States). The membranes were blocked with 5% skim milk and incubated overnight with the primary antibodies at 4 °C (Table 2). Then, the membranes were incubated with horseradish peroxidase-conjugated anti-mouse (sc-516102, Santa Cruz Biotechnology, 1:10000) or anti-rabbit (sc-2357, Santa Cruz Biotechnology, 1:10000) antibodies overnight or for 5 h. The enhanced chemiluminescence reagent was used to develop the membranes, and images were captured using an imager. Quantum One software (Bio-Rad) and Image J software (NIH) were used to quantify the expression levels of the proteins. The relative protein expression was reflected as the gray value of the proteins, and glyceraldehyde 3 phosphate dehydrogenase (GAPDH) was used as the internal control.

Malondialdehyde detection

Malondialdehyde (MDA) represents the end result of lipid peroxidation and can indirectly indicate the extent of free radical damage in the liver[40]. The levels of MDA were determined using the thiobarbituric acid test, according to the MDA test kit instructions (cargo number: AOO 3-1; Nanjing Jiancheng, Nanjing, Jiangsu Province, China). Four types of tubes, namely a blank tube, a standard tube, sample tubes, and a control tube, were each filled with 0.1 mL of absolute alcohol, standard (10 nmol/mL tetraethyl propane), the sample to be tested, and reagent I, respectively. Subsequently, the tubes were shaken to mix the samples and reagents. Next, 1.5 mL each of reagent II, reagent III, and 50% glacial acetic acid were added to the test tubes in that order, according to the kit instructions. The contents were thoroughly mixed using a vortex mixer and boiled for 40 min with the lid on. After cooling under running water, the tubes were centrifuged at 3500-4000 rpm for 10 min. Following this, 0.2 mL of the resulting supernatant was transferred to each well of a 96-well plate. The optical density (OD) at 532 nm was measured using an enzyme-labeled instrument (Gene Technology Co. Ltd., Shanghai, China), and the protein concentration (mg/mL) was determined based on the standard curve. Finally, the MDA content in the liver tissue was calculated using the formula: Hepatic tissue MDA content (nmol/mg protein) = [(measured OD-control OD)/(standard OD-blank OD)] × (standard concentration/protein concentration of the sample being tested).

Measurement of liver triglyceride and total cholesterol levels

The liver triglyceride (TG) and total cholesterol (TC) levels were determined using the TG content assay kit (AKFA003C, Boxbio, Beijing, China) and the TC content assay kit (AKFA002C, Boxbio, China), respectively. Sample preparation and addition were carried out according to the instructions of the assay kits. The absorbance of TG and TC was measured at the wavelengths of 420 nm and 500 nm, respectively, by using an enzyme-labeled instrument (Gene Technology Co. Ltd., Shanghai, China). The TG and TC contents in the liver were calculated based on the instructions of the assay kits.

Statistical analysis

Statistical analysis was conducted using SPSS 29.0 (IBM, Chicago, IL, United States). Continuous variables that conformed to a normal distribution were analyzed using the one-sample Kolmogorov-Smirnov test, and expressed as means and standard deviations. An independent *t*-test analysis was used for comparisons between two groups. One-way analysis of variance was used to determine the statistical significance of comparisons among multiple groups, and if statistically significant differences were identified, post hoc pairwise comparisons were further performed using the least significant difference *t* test method. A *P* value of less than 0.05 was considered statistically significant.

RESULTS

UGT1A1 mutation or low UGT1A1 level is closely associated with liver damage

The genetic sequencing results of a total of 7 patients were included in this study. The results revealed mutations at different sites of the *UGT1A1* gene (Figure 1A-G). The results of liver-function tests indicated that the patients had elevated levels of TBil, mainly IBil (Table 3). Patients 1 and 2 exhibited signs of liver cirrhosis on abdominal magnetic resonance imaging (Figure 1A and B). Histopathological examination of the liver indicated varying degrees of chronic inflammatory changes in patients 3, 4, 5, and 6 (Figure 1C-F). Patient 7 did not undergo liver puncture biopsy, so we were unable to examine his pathology results. Proteomics analysis suggested differential expression of UGT1A1 in patients with ACLF, with significantly decreased intrahepatic UGT1A1 expression as compared to patients with chronic hepatitis ($P < 0.05$; Figure 1H).

Hepatic UGT1A1 protein level is increased in mice with CCl_4-induced liver injury

At 12 h, 24 h, 48 h, and 72 h after CCl_4-induced liver injury, the serum ALT and TBil levels in mice were significantly higher than the levels in the 0 h (control) group. The ALT level peaked at 24 h, while the TBil level peaked at 48 h in the CCl_4 group ($P < 0.01$; Figure 2A and B). The area of liver-tissue necrosis expanded over time, and the necrotic liver cells were predominantly located around the central vein zone ($P < 0.01$; Figure 2C and E). Liver-cell apoptosis also increased over time, and the apoptotic index peaked at 24 h ($P < 0.01$; Figure 2D and E). Compared with the 0 h group, the CCl_4 groups showed significantly increased protein levels of UGT1A1, cleaved caspase-3, and phosphorylated MLKL (p-MLKL, $P < 0.01$; Figure 2F and G). The level of UGT1A1 peaked at 48 h, while the levels of cleaved caspase-3 and p-MLKL peaked at 24 h after the CCl_4 injection.

Hepatic UGT1A1 protein level is increased in mice with ConA-induced liver injury

Compared to the 0 h (control) group, the ConA groups showed significantly increased serum levels of ALT and TBil at 12 h, 24 h, and 48 h after the induction of liver injury. The ALT level peaked at 24 h, while the TBil level peaked at 48 h ($P < 0.01$; Figure 3A and B). The area of liver-tissue necrosis expanded over time, and the necrotic liver cells were mainly located around the portal areas ($P < 0.01$; Figure 3C and E). Liver-cell apoptosis also increased over time, and the apoptotic index peaked at 24 h ($P < 0.01$; Figure 3D and E). Compared to the control group, the ConA group showed significantly increased protein expression levels of UGT1A1, cleaved caspase-3, and p-MLKL ($P < 0.01$; Figure 3F and G), with the cleaved caspase-3 and p-MLKL levels peaking at 24 h after the injection of ConA solution.

LPS exacerbated CCl_4-induced liver injury and decreased hepatic UGT1A1 expression in mice

Compared to the control group treated with CCl_4 alone, the LPS + CCl_4 group showed significantly increased serum levels of ALT and TBil. Additionally, the area of liver-tissue necrosis and the hepatocyte apoptotic index were increased ($P < 0.01$; Figure 4A-E). Western blot analysis showed that the expression levels of UGT1A1 in mice were decreased in the LPS + CCl_4 group relative to the control group, while those of cleaved caspase-3 and p-MLKL were significantly increased ($P < 0.01$; Figure 4F and G).

Liver steatosis worsens CCl_4-induced liver injury and reduces hepatic UGT1A1 protein levels in mice

Compared to mice with chronic liver injury induced by CCl_4 alone, mice in the CCl_4 + HFD group exhibited a significant increase in the levels of ALT and TBil at 24 h ($P < 0.01$; Figure 5A and B). Additionally, the area of liver-tissue necrosis ($P < 0.01$; Figure 5C and E) and the hepatocyte apoptotic index were increased ($P < 0.01$; Figure 5D and E), indicating that hepatic steatosis led to the progression of liver injury in the mouse model. In mice with progress of liver injury (*i.e.*, the CCl_4 + HFD group), the hepatic expression of UGT1A1 protein was decreased, while the expressions of cleaved caspase-3 and p-MLKL were significantly increased ($P < 0.01$; Figure 5F and G).

Ugt1a1 KO worsened CCl_4-induced liver injury in mice

Model mice were transfected with rAAV8 carrying control sgRNA, *Ugt1a1* sgRNA1, *Ugt1a1* sgRNA2, or *Ugt1a1* sgRNA3. At 6 wk after transfection, the expression level of UGT1A1 was measured using Western blot analysis. The results showed that the hepatic UGT1A1 expression was decreased in mice transfected with *Ugt1a1* sgRNA2 and *Ugt1a1* sgRNA3, and the decrease was more significant in the *Ugt1a1* sgRNA2 group. Therefore, we selected *Ugt1a1* sgRNA2 as the specific *Ugt1a1* sgRNA for the KO of the *Ugt1a1* gene ($P < 0.01$; Figure 6A). The study aimed to investigate the role and mechanism of UGT1A1 in liver injury by utilizing *Ugt1a1*-KO mice with acute and chronic liver injury. No mortalities were observed in the models involving acute liver injury. However, in the case of the chronic liver injury models, 3 mice in the *Ugt1a1*-KO group died, resulting in a mortality rate of 25%. In both the acute and chronic liver injury models involving *Ugt1a1*-KO, the *Ugt1a1*-KO + CCl_4 group exhibited significant increases in the serum ALT and TBil levels (mainly IBil level), relative to the CCl_4 group ($P < 0.01$; Figure 6B, C, I, and J). The *Ugt1a1*-KO + CCl_4 group also showed increased liver-tissue necrotic area, more pronounced liver fibrosis on Masson trichrome staining ($P < 0.01$; Figure 6D, F, K, and M), and a significant increase in the apoptotic index ($P < 0.01$; Figure 6E, F, L, and M). Moreover, the hepatic level of UGT1A1 protein was decreased, while the levels of cleaved caspase-3 and p-MLKL were significantly elevated ($P < 0.01$; Figure 6G, H, N, and O).

Ugt1a1 KO worsened ConA-induced liver injury in mice

Compared to the ConA group, the *Ugt1a1*-KO + ConA group showed greater increases in the serum ALT and TBil levels

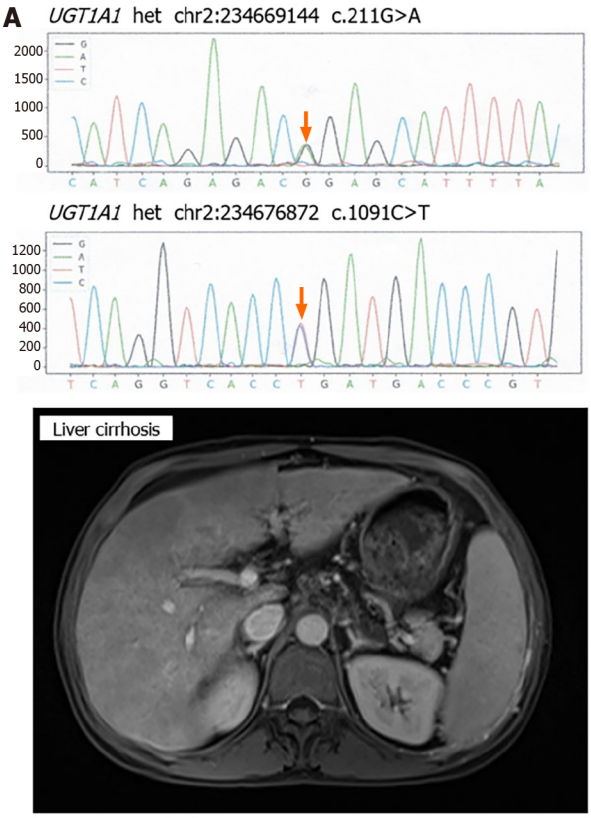
A
UGT1A1 het chr2:234669144 c.211G>A
UGT1A1 het chr2:234676872 c.1091C>T
Liver cirrhosis

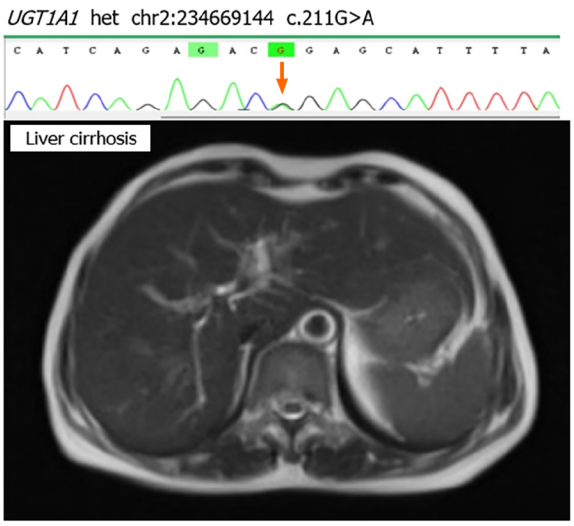
B
UGT1A1 het chr2:234669144 c.211G>A
Liver cirrhosis

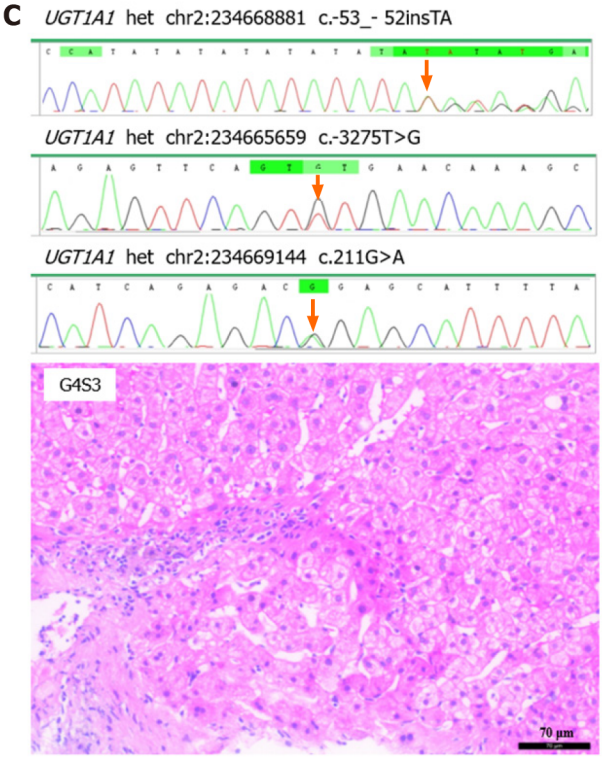
C
UGT1A1 het chr2:234668881 c.-53_- 52insTA
UGT1A1 het chr2:234665659 c.-3275T>G
UGT1A1 het chr2:234669144 c.211G>A
G4S3
70 μm

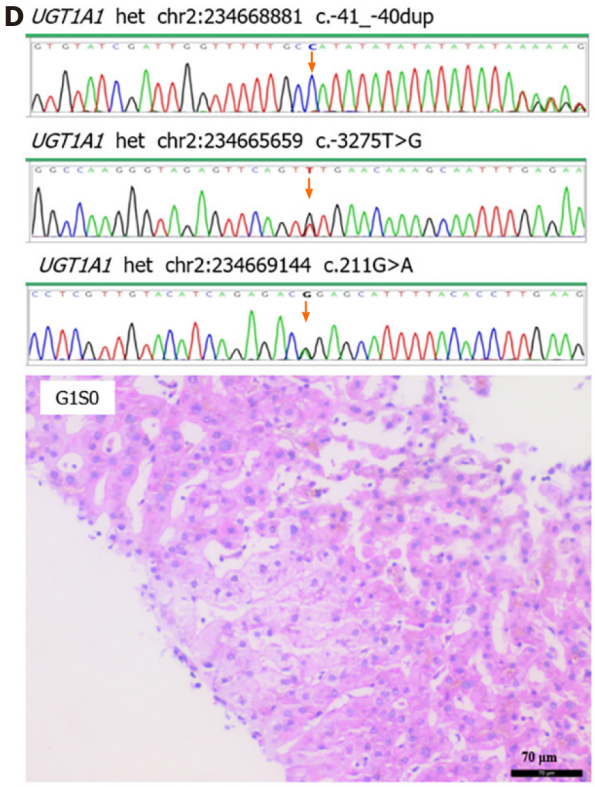
D
UGT1A1 het chr2:234668881 c.-41_-40dup
UGT1A1 het chr2:234665659 c.-3275T>G
UGT1A1 het chr2:234669144 c.211G>A
G1S0
70 μm

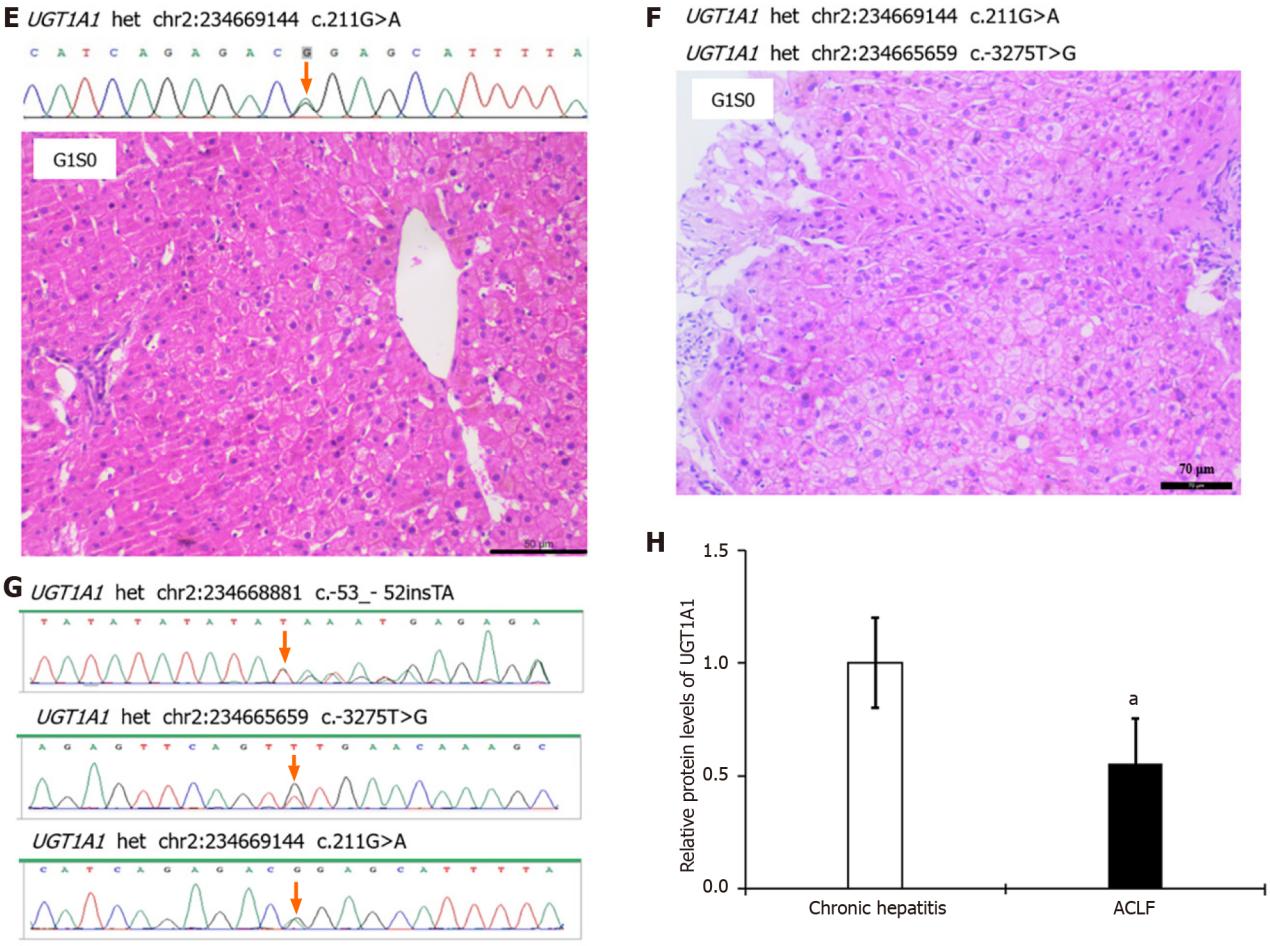

Figure 1 *Uridine diphosphate glucuronosyltransferase 1A1* gene mutation is closely associated with liver injury. A-G: The uridine diphosphate glucuronosyltransferase 1A1 (*UGT1A1*) gene sequencing, imaging, and pathological biopsy results for patients 1 to 7; H: Relative protein levels of *UGT1A1* in chronic hepatitis and acute-on-chronic liver failure. $^{a}P < 0.05$ *vs* the chronic hepatitis group. UGT1A1: Uridine diphosphate glucuronosyltransferase 1A1.

(mainly in the IBil level), the area of necrotic liver tissue, and the hepatocyte apoptotic index ($P < 0.01$; Figure 7A-E). Additionally, the latter group showed significant reduction in the protein expression of UGT1A1, and elevations in the protein expressions of cleaved caspase-3 and p-MLKL in the liver ($P < 0.01$; Figure 7F and G).

Interference with upregulation of UGT1A1 exacerbates hepatic ER stress, oxidative stress, and lipid metabolism disorder during liver injury

The hepatic MDA, TG, and TC contents in the mice with CCl_4-induced liver injury were increased as compared with the 0 h group ($P < 0.01$; Figure 8A-C). The hepatic expressions of the ER stress-related protein 78-kDa glucose-regulated protein (GRP78) and the oxidative stress-related protein uncoupling protein-2 (UCP2) were also higher in the CCl_4 groups than in the 0 h group ($P < 0.01$). Additionally, the expressions of the lipid metabolism-related proteins microsomal TG transfer protein (MTP, which participates in lipid excretion) and medium-chain acyl-CoA dehydrogenase (MCAD, which participates in fatty acid β-oxidation) were decreased, and the expressions of the transcription factor cleaved sterol regulatory element-binding protein 1 (SREBP1c, which participates in lipid synthesis) and acyl-CoA synthetase long chain family member 4 (ACSL4, which promotes lipid peroxidation) were increased ($P < 0.01$; Figure 8D). Compared to the CCl_4 group, the *Ugt1a1*-KO + CCl_4 group exhibited a significant increase in the hepatic MDA, TG, and TC contents ($P < 0.01$; Figure 8E-G). The GRP78 and UCP2 levels were further elevated, and the decrease in the MTP level was more significant; the levels of SREBP1c and ACSL4 were significantly increased, and the level of MCAD was unchanged ($P < 0.01$; Figure 8H).

Similarly, in mice with ConA-induced liver injury, the hepatic MDA, TG, and TC contents ($P < 0.05$; Figure 8I-K), and the hepatic expressions of GRP78 and UCP2 were all increased, while the expressions of MTP and MCAD were decreased; the expressions of SREBP1c and ACSL4 were increased ($P < 0.01$; Figure 8L). Compared with the ConA group, the *Ugt1a1*-KO + ConA group exhibited significant increases in the hepatic MDA, TG, and TC contents ($P < 0.01$; Figure 8M-O), further elevation of the GRP78 and UCP2 Levels, and a more significant decrease in the MTP level; the levels of SREBP1c and ACSL4 were significantly increased, and the level of MCAD was unchanged ($P < 0.01$; Figure 8P).

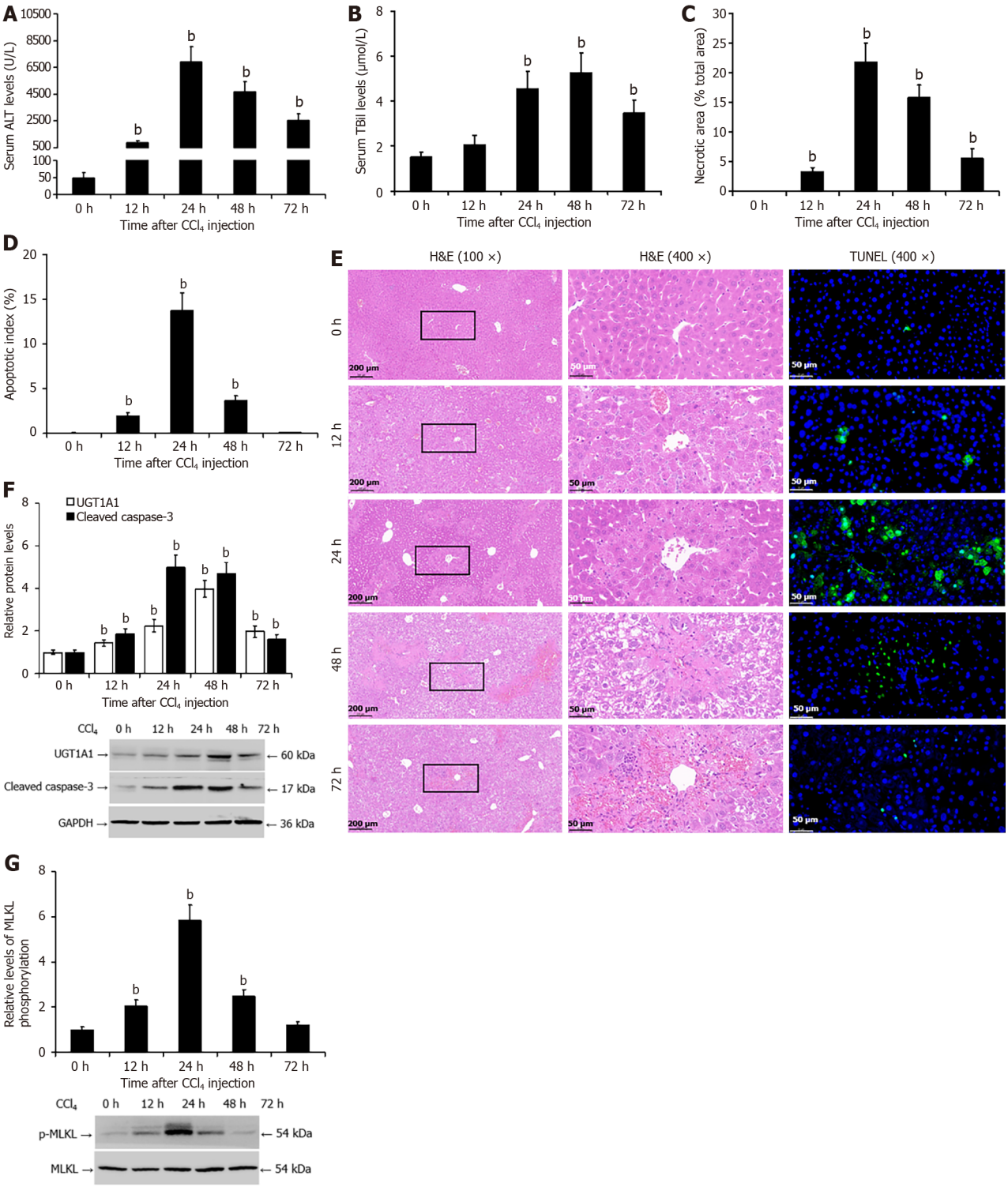

Figure 2 Increased uridine diphosphate glucuronosyltransferase 1A1 protein levels in the livers of mice with carbon tetrachloride-induced liver injury. A: The enzyme rate method was used to detect the serum level of alanine transaminase in mice; B: The diazo method was used to detect the serum total bilirubin level; C and E: Pathological analysis of liver tissue by hematoxylin and eosin staining; D and E: Terminal deoxynucleotidyl transferase-mediated deoxyuridine triphosphate-nick end labelling assay was used to measure hepatocyte apoptosis; F: Western blotting was used to detect the protein levels of uridine diphosphate glucuronosyltransferase 1A1 and cleaved caspase-3; G: Western blotting was used to detect the protein levels of phosphorylated mixed lineage kinase domain-like pseudokinase. $^{b}P < 0.01$ *vs* the 0 h (control) group. UGT1A1: Uridine diphosphate glucuronosyltransferase 1A1; ALT: Alanine transaminase; TBil: Total bilirubin; H&E: Hematoxylin and eosin; TUNEL: Transferase-mediated deoxyuridine triphosphate-nick end labelling; p-MLKL: Phosphorylated mixed lineage kinase domain-like pseudokinase; CCl_4: Carbon tetrachloride; GAPDH: Glyceraldehyde 3 phosphate dehydrogenase.

DISCUSSION

This study focuses on the effects of UGT1A1 on the progression of liver injury and the mechanisms underlying these effects. Through clinical research and animal experiments, we discovered that patients with *UGT1A1* gene mutations had varying degrees of liver injury, and patients with ACLF had relatively decreased hepatic UGT1A1 expression, as compared to patients with chronic hepatitis. In a mouse model of liver injury, the hepatic expression of UGT1A1 was increased, while in mouse models of liver injury induced by CCl_4 and worsened by LPS or hepatosteatosis, the hepatic expression of UGT1A1 was significantly decreased as compared to the control groups induced solely by CCl_4. These findings are consistent with the observations in the patients with ACLF. *Ugt1a1* KO exacerbated liver injury, heaptocyte apoptosis, and necroptosis in the mouse model and worsened hepatocyte ER stress, oxidative stress, and lipid metabolism disorders. The above results indicate that the expression of UGT1A in hepatocytes is upregulated as a compensatory mechanism during liver injury. The upregulation of UGT1A1 is beneficial for hepatocytes to avoid apoptosis and necroptosis under conditions of ER stress, oxidative stress, and disrupted lipid metabolism. When this compensatory upregulation of UGT1A1 is disrupted during liver injury due to, for example, gene mutations, concomitant endotoxemia, or hepatic steatosis, the progression of liver damage may be accelerated.

Insertion and deletion mutations, and single-nucleotide polymorphisms of the *UGT1A1* gene can greatly affect the metabolism of endogenous and exogenous substances[41]. Thus far, research on *UGT1A1* polymorphisms has focused on endogenous bilirubin metabolism and exogenous drug metabolic detoxification, and especially on disorders in bilirubin metabolism since UGT1A1 is a liver enzyme that primarily metabolizes glucuronidated bilirubin[4,41]. The most common congenital genetic diseases involving *UGT1A1* are GS and Crigler-Najjar syndrome (CNS)[42]. GS and CNS are characterized by the partial and complete deficiency of UGT1A1 enzyme activity, respectively. In GS patients, the UGT1A1 enzyme activity is reduced to approximately 30% of normal, and the clinical symptoms are mild. However, in type I CNS patients, the UGT1A1 enzyme activity is severely deficient or even absent, leading to severe jaundice and a high risk of progression to kernicterus, with a very high mortality rate[43]. GS is most commonly seen in patients with hereditary hyperbilirubinemia, with a high incidence rate of 2%-10%[44]. GS is a common autosomal dominant genetic disorder, and mutations in the promoter region of the *UGT1A1* gene are an important genetic basis for the development of GS. The frequency distribution of mutant alleles in the promoter sequence of the *UGT1A1* gene varies among different populations, with a frequency of up to 36% in African populations, only 3% in Asian populations, and as low as 0.13% in Japan[45]. At present, the most studied mutations are UGT1A1*6 and UGT1A1*28. The polymorphism of the UGT1A1*6 Locus is represented by 211 G>A, forming 3 genotypes: G/G, A/G, and A/A, which are prevalent in Asian populations [46]. UGT1A1*28 consists of a sequence of 7 TA repeats, including homozygous and heterozygous mutations[47]. In this study, we included 7 patients in the clinical study, all of whom had 1 or more mutations in the *UGT1A1* gene. All 7 patients had a mutation at the UGT1A1*6 site, and 2 patients had a mutation at the UGT1A1*28 site. Additionally, all 7 patients showed elevated levels of unconjugated bilirubin (UCB), which is consistent with the characteristics of GS. GS is believed to be a benign disease that does not require treatment[44]. However, in our study, patients with *UGT1A1* mutations had varying degrees of chronic inflammatory changes in the liver. UGT1A1 expression was decreased in patients with ACLF as compared to patients with chronic hepatitis, suggesting that *UGT1A1* mutation or low levels of UGT1A1 may be associated with liver injury. In the animal experiments, we found that UGT1A1 protein levels were upregulated in the livers of mice with liver injury induced by CCl_4 or ConA. However, in mice with CCl_4-induced severe liver injury worsened by LPS or hepatic steatosis, the UGT1A1 Levels were decreased, and hepatocyte apoptosis and necroptosis were exacerbated. Most importantly, liver injury was aggravated after *Ugt1a1* KO. These results indicate that UGT1A1 is upregulated as compensatory response after liver injury, and UGT1A1 deficiency or suppressed expression may contribute to the progression of liver injury.

Impaired bilirubin metabolism is one of the characteristics of liver injury[48]. High concentrations of UCB cause severe neurological damage and cell death associated with kernicterus[49], and lead to the cytoplasmic vacuolation of liver cells and bile duct congestion[11]. Studies have confirmed the close relationship of ER stress, oxidative stress, and lipid metabolism disorders in liver cells with the progression of liver injury[50,51]. To further clarify the role of UGT1A1 in liver injury, we will analyze and discuss its effects and related mechanisms from 3 perspectives: ER stress, oxidative stress, and lipid metabolism.

When cellular homeostasis is disrupted, ER stress is activated[52]. ER stress is mediated by the coordinated pathways of inositol-requiring enzyme 1, activating transcription factor 6 (ATF6), and protein kinase R-like ER kinase[53]. ATF6, ATF4, and other transcription factors can increase the expression of molecular chaperones during ER stress. This facilitates the processing of proteins and maintains normal cell function. However, if ER stress persists or becomes excessive, it can trigger signals such as apoptosis and necroptosis, leading to damage responses[54]. GRP78 is a molecular chaperone in the ER, where it is a marker for ER stress activation[55]. When liver damage and *UGT1A1* mutation coexist, the elevation in the level of IBil (*i.e.*, UCB) will be more significant, and high levels of IBil can worsen hepatocyte ER stress [56]. Studies have reported that UCB activates ER stress and promotes cell apoptosis[57]. UCB has also been found to activate ER stress in the neurons, promoting cellular inflammation and apoptosis. Four-Phenylbutyric acid is an inhibitor of ER stress, and can alleviate UCB-induced cell apoptosis[58]. Furthermore, the research by Schiavon *et al*[59] has indicated that UCB activates the nuclear factor kappa-B (NF-κB) pathway *in vitro*, leading to the mediation of inflammatory responses. Our preliminary research found that ER stress activates the apoptosis and necroptosis of liver cells in the setting of acute liver injury[60,61]. *In vitro* studies have revealed that UCB intervention increases the apoptosis and necroptosis of oligodendrocyte precursor cells[58]. In this study, we found that the UGT1A1 expression was downregulated, and the UCB level was elevated in mice with SAE of liver injury. *Ugt1a1* KO worsened hepatic ER stress, which was confirmed by elevated GRP78 Levels, and resulted in the increased apoptosis and necroptosis of the liver cells. This suggests that the disruption of UGT1A1 upregulation during liver injury worsens ER stress, exacerbates the apoptosis

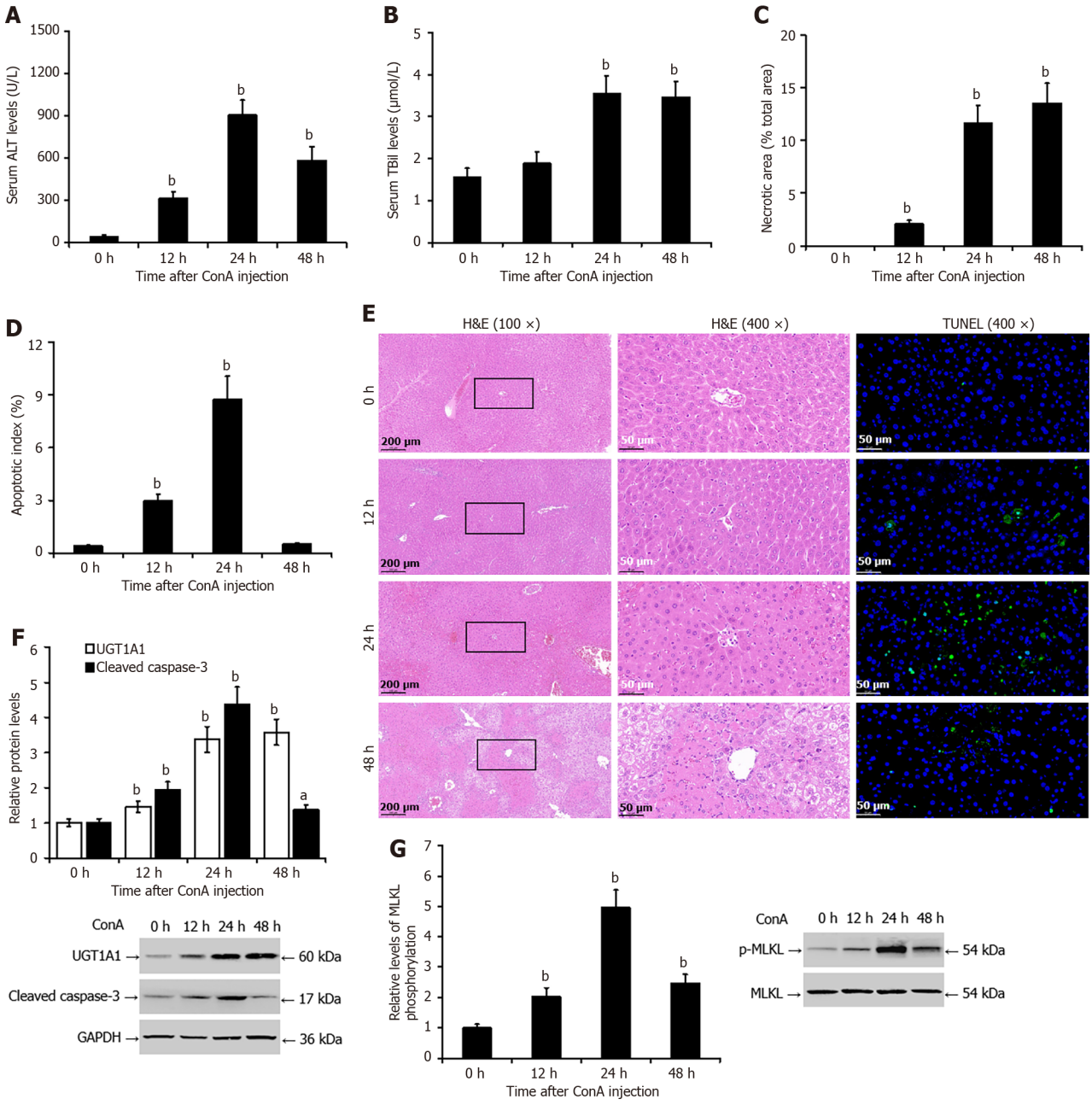

Figure 3 Increased levels of uridine diphosphate glucuronosyltransferase 1A1 protein in the livers of mice with concanavalin A-induced liver injury. A: The enzyme rate method was used to detect the serum level of alanine transaminase in mice; B: The diazo method was used to detect the serum level of total bilirubin; C and E: Pathological analysis of liver tissue by hematoxylin and eosin staining; D and E: terminal deoxynucleotidyl transferase-mediated deoxyuridine triphosphate-nick end labelling assay was used to measure hepatocyte apoptosis; F: Western blotting was used to detect the protein levels of uridine diphosphate glucuronosyltransferase 1A1 and cleaved caspase-3; G: Western blotting was used to detect the protein levels of phosphorylated mixed lineage kinase domain-like pseudokinase. $^{b}P < 0.01$ *vs* the 0 h (control) group. UGT1A1: Uridine diphosphate glucuronosyltransferase 1A1; ALT: Alanine transaminase; TBil: Total bilirubin; H&E: Hematoxylin and eosin; TUNEL: Transferase-mediated deoxyuridine triphosphate-nick end labelling; p-MLKL: Phosphorylated mixed lineage kinase domain-like pseudokinase; ConA: Concanavalin A; GAPDH: Glyceraldehyde 3 phosphate dehydrogenase.

and necroptosis of liver cells, and accelerates the progression of liver injury.

Oxidative stress is a stress response that results from the excessive production of reactive oxygen species (ROS) and the relatively low activity of antioxidants[62,63]. These changes result in mitochondrial dysfunction and promote cell apoptosis[64]. ROS production has been found to simultaneously mediate ER stress and mitochondrial dysfunction, which collectively promote liver-disease progression[65]. UCP2 is a member of the superfamily of anion carriers in the inner mitochondrial membrane; it prevents mitochondrial oxidative damage, and is upregulated during oxidative stress [66]. A study investigating the effects of bilirubin-induced apoptosis in mouse liver cancer cells revealed that high doses of UCB disrupt the cellular energy metabolism and result in excessive ROS production within the cells[67]. A study on the toxicity of UCB-induced liver cancer cells in mice found that approximately 3.5 h after exposing the mouse liver cancer cells to 50 μmol/L UCB, the classical cell apoptosis-related protein caspase-9 was activated; additionally, the UCB-mediated apoptosis of liver cancer cells was associated with increased oxidative stress[68]. UCB may interfere with the

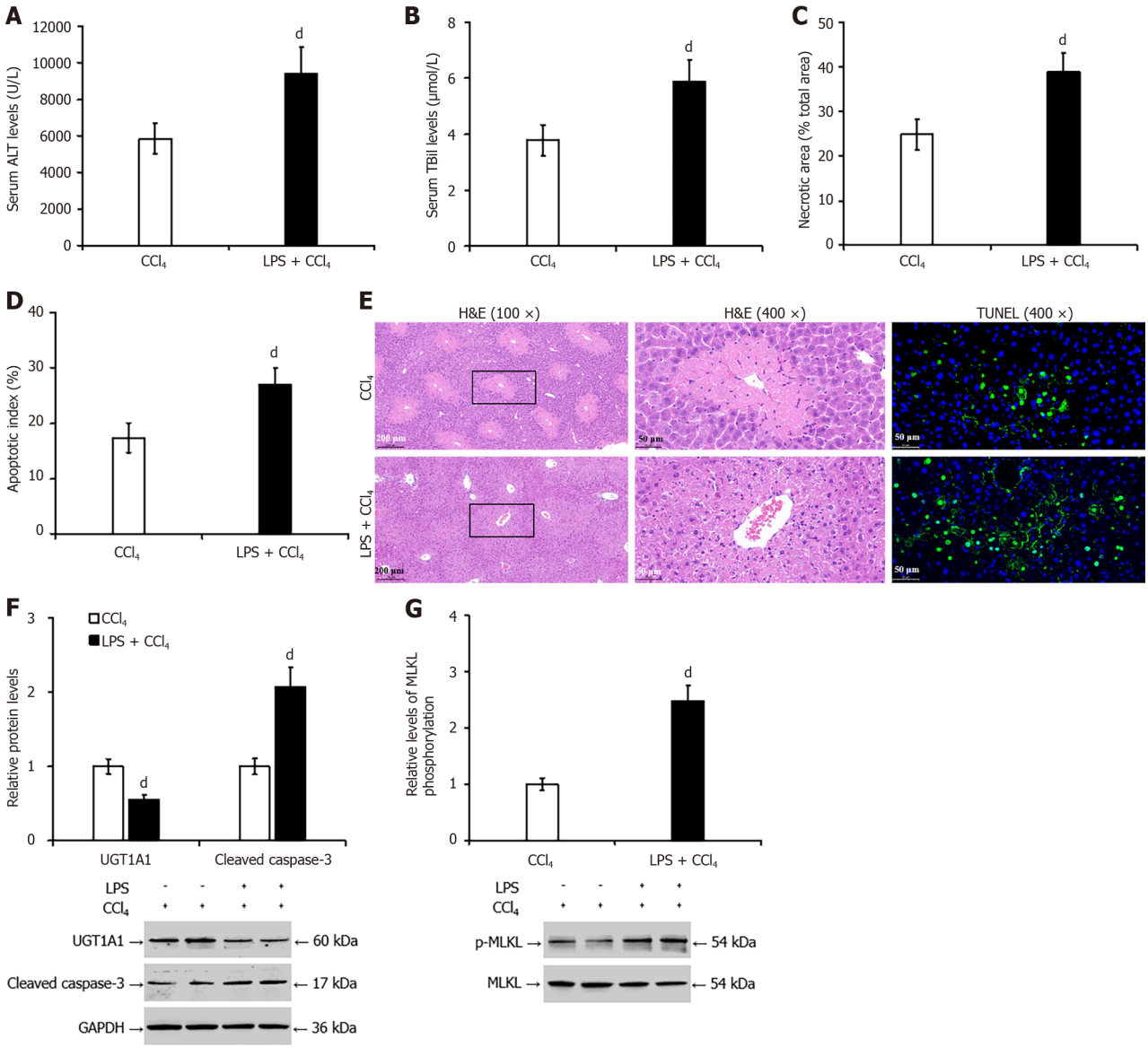

Figure 4 Lipopolysaccharide exacerbated carbon tetrachloride-induced liver injury in mice and decreased hepatic uridine diphosphate glucuronosyltransferase 1A1 expression. A: The enzyme rate method was used to detect the serum levels of alanine transaminase in mice; B: Pathological analysis of liver tissue by hematoxylin and eosin staining; C and E: The terminal deoxynucleotidyl transferase-mediated deoxyuridine triphosphate-nick end labelling assay was used to measure hepatocyte apoptosis; D and E: The diazo method was used to detect the serum level of total bilirubin; F: Western blotting was used to detect the protein levels of uridine diphosphate glucuronosyltransferase 1A1 and cleaved caspase-3; G: Western blotting was used to detect the protein levels of phosphorylated mixed lineage kinase domain-like pseudokinase. $^{d}P < 0.01$ *vs* the carbon tetrachloride group. UGT1A1: Uridine diphosphate glucuronosyltransferase 1A1; ALT: Alanine transaminase; TBil: Total bilirubin; H&E: Hematoxylin and eosin; TUNEL: Transferase-mediated deoxyuridine triphosphate-nick end labelling; p-MLKL: Phosphorylated mixed lineage kinase domain-like pseudokinase; CCl_4: Carbon tetrachloride; LPS: Lipopolysaccharide; GAPDH: Glyceraldehyde 3 phosphate dehydrogenase.

mitochondrial electron transport chain, release the constraints of oxidative phosphorylation, cause mitochondrial membrane potential collapse, and thereby initiate apoptosis[69]. Another study has found that bilirubin-induced oxidative stress causes deoxyribonucleic acid (DNA) damage in human neuroblastoma cells[49]. High ROS levels during hyperbilirubinemia can promote neuronal cell apoptosis through the phosphorylation of P38 and the activation of caspase-3[70]. The oxidative stress generated by elevated UCB concentrations is thus a key mechanism underlying bilirubin-induced cell toxicity[70,71]. Liu *et al*[13] have also indicated that the reduction of UGT1A1 increases susceptibility to liver injury and exacerbates liver damage; bilirubin-induced oxidative stress and DNA damage are significant factors that cause liver-cell injury. Their research also suggests that the accumulation of bilirubin activates the NF-κB signaling pathway, initiating cellular inflammation and immune responses, thereby inducing liver-cell damage. Many studies have shown that oxidative stress can lead to mitochondrial apoptosis and necroptosis[72,73]. Our research indicates that hepatic oxidative stress is increased when *Ugt1a1* is knocked out, as demonstrated by the elevated levels of MDA and UCP2 in the animal experiments. This suggests that low levels of UGT1A1 exacerbate oxidative stress during liver injury.

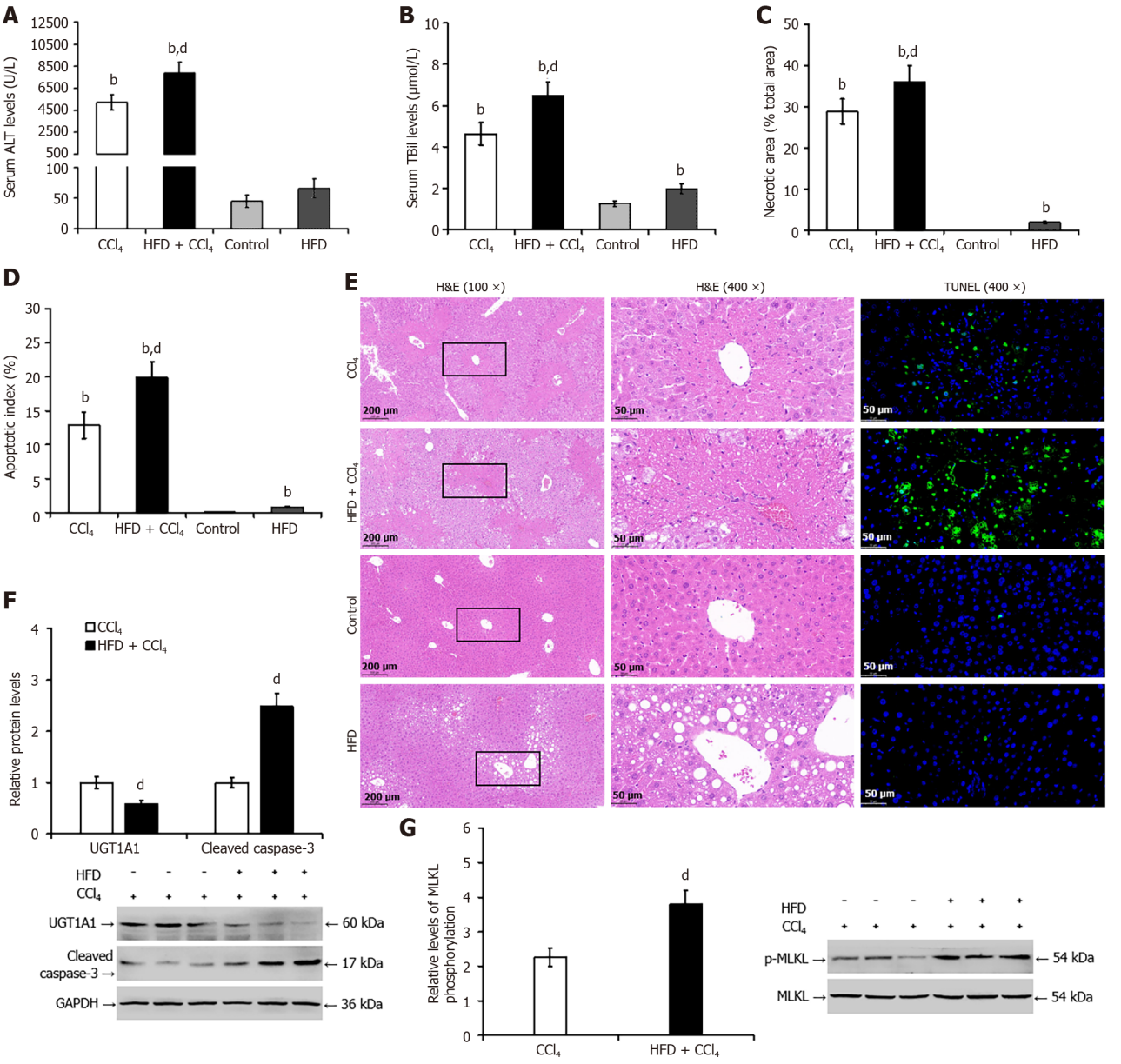

Figure 5 Liver steatosis worsens carbon tetrachloride-induced liver injury and reduces hepatic uridine diphosphate glucuronosyltransferase 1A1 protein levels in mice. A: The enzyme rate method was used to detect the serum level of alanine transaminase in mice; B: The diazo method was used to detect the serum level of total bilirubin; C and E: Pathological analysis of liver tissue by hematoxylin and eosin staining; D and E: The terminal deoxynucleotidyl transferase-mediated deoxyuridine triphosphate-nick end labelling assay was used to measure hepatocyte apoptosis; F: Western blotting was used to detect the protein levels of uridine diphosphate glucuronosyltransferase 1A1 and cleaved caspase-3; G: Western blotting was used to detect the protein levels of phosphorylated mixed lineage kinase domain-like pseudokinase. $^{b}P < 0.01$ *vs* the control group; $^{d}P < 0.01$ *vs* the carbon tetrachloride group. UGT1A1: Uridine diphosphate glucuronosyltransferase 1A1; ALT: Alanine transaminase; TBil: Total bilirubin; H&E: Hematoxylin and eosin; TUNEL: Transferase-mediated deoxyuridine triphosphate-nick end labelling; p-MLKL: Phosphorylated mixed lineage kinase domain-like pseudokinase; CCl_4: Carbon tetrachloride; HFD: High-fat diet; GAPDH: Glyceraldehyde 3 phosphate dehydrogenase.

UGT1A1, as an important member of the uridine diphosphate glucuronyltransferase metabolic enzyme superfamily, can directly participate in the metabolism of unsaturated fatty acids such as arachidonic acid and linoleic acid[74]. In addition, UGT1A1 indirectly affects lipid metabolism through its influence on ER stress and oxidative stress in liver cells [75]. Research has shown that all 3 branches of the unfolded protein response (UPR) are involved in the regulation of lipid metabolism[33,76], and that a sustained and severe UPR exacerbates the disruption of lipid metabolism and worsens hepatocyte lipid degeneration[77,78]. MTP promotes the transfer of lipids to apolipoprotein B, a nascent lipoprotein, resulting in the formation of the precursor particles of very-low-density lipoprotein[79]. The inhibition of MTP activity can disrupt the assembly and secretion of very-low-density lipoprotein-TGs, causing the accumulation of TGs in the liver and resulting in hepatic steatosis[80]. MCAD is a medium-chain fatty acid oxidase, and MCAD deficiency is one of the most common mitochondrial fatty acid β-oxidation disorders[81]. MCAD deficiency prevents the dehydrogenation step of β-oxidation in the mitochondria, leading to decreased acetyl-CoA production and the accumulation of acylcarnitine caused by carnitine transport from medium-chain fatty acids, resulting in disorders of intrahepatic lipid metabolism[82]. SREBP1c is a key adipogenic transcription factor that is activated by insulin in the postprandial state. It regulates the

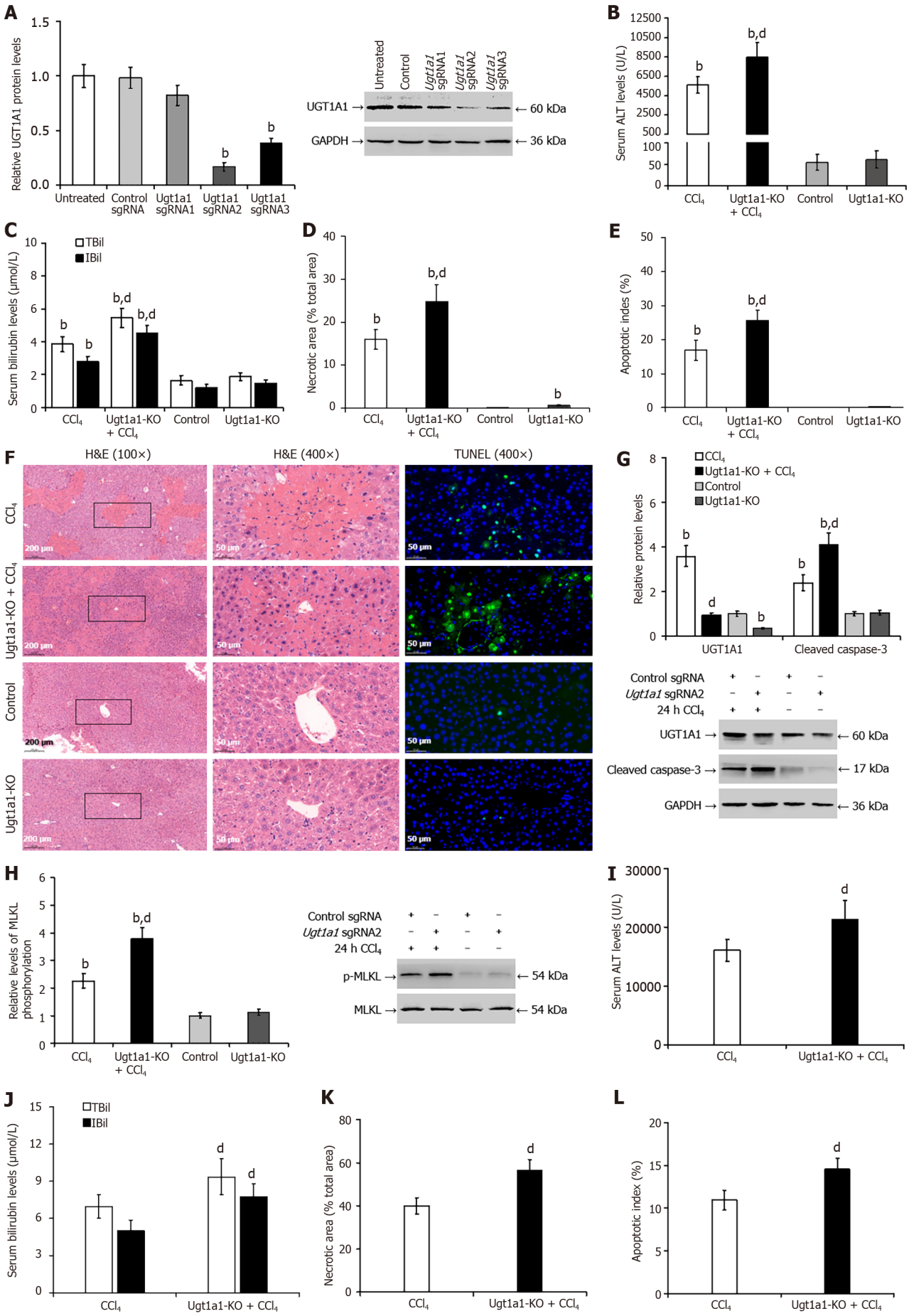
A
Relative UGT1A1 protein levels
Untreated
Control sgRNA
Ugt1a1 sgRNA1
Ugt1a1 sgRNA2
Ugt1a1 sgRNA3
UGT1A1
GAPDH
60 kDa
36 kDa
B
Serum ALT levels (U/L)
CCl4
Ugt1a1-KO + CCl4
Control
Ugt1a1-KO
C
Serum bilirubin levels (μmol/L)
TBil
IBil
D
Necrotic area (% total area)
E
Apoptotic index (%)
F
H&E (100×)
H&E (400×)
TUNEL (400×)
CCl4
Ugt1a1-KO + CCl4
Control
Ugt1a1-KO
200 μm
50 μm
G
Relative protein levels
UGT1A1
Cleaved caspase-3
Control sgRNA
Ugt1a1 sgRNA2
24 h CCl4
17 kDa
H
Relative levels of MLKL phosphorylation
p-MLKL
MLKL
54 kDa
I
Serum ALT levels (U/L)
J
Serum bilirubin levels (μmol/L)
K
Necrotic area (% total area)
L
Apoptotic index (%)

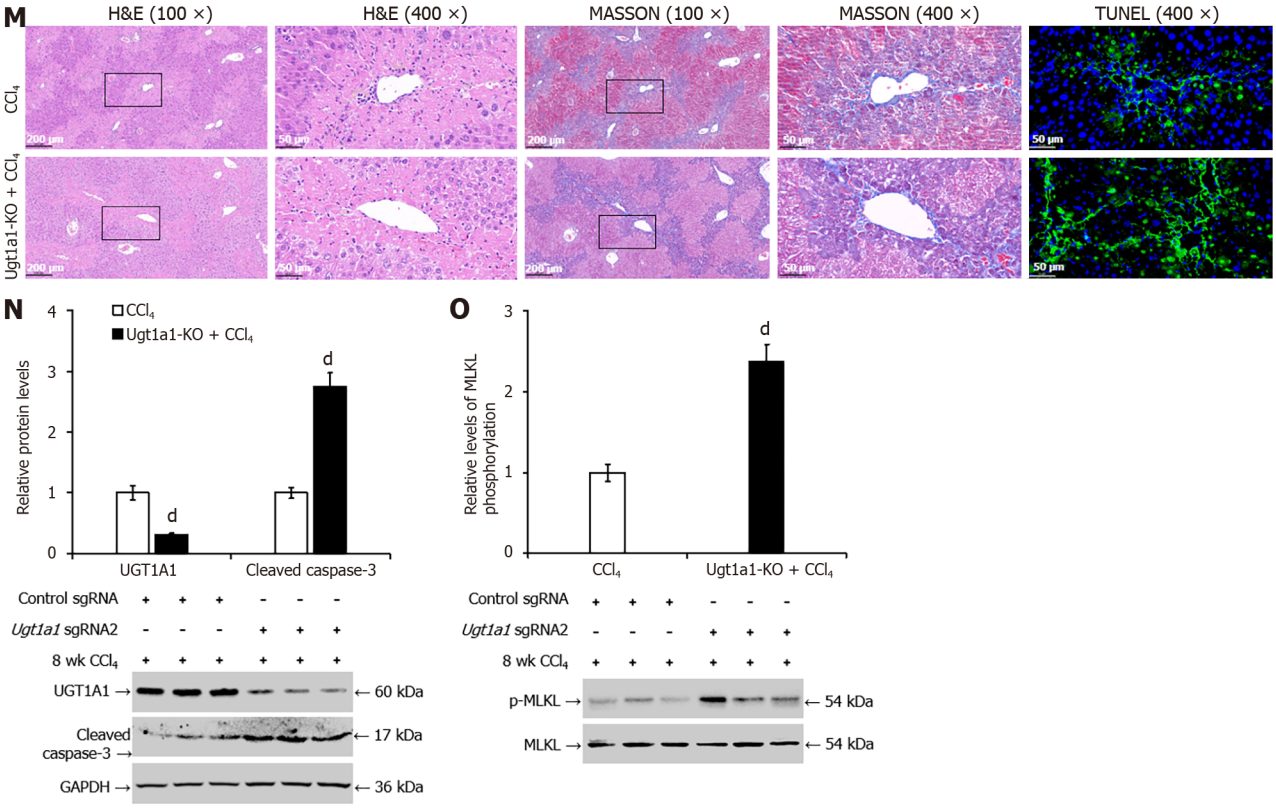

Figure 6 Knocking out uridine diphosphate glucuronosyltransferase 1A1 worsened carbon tetrachloride-induced liver injury in mice. A: Western blotting was utilized to screen for the specific *Ugt1a1* sgRNA that induced *Ugt1a1* gene knockout; B and I: The enzyme rate method was used to detect the serum level of alanine transaminase in mice; C and J: The diazo method was used to detect the serum levels of total bilirubin and indirect bilirubin; D, F, K, and M: Pathological analysis of liver tissue by hematoxylin and eosin (H&E) and Masson staining; E, F, L, and M: The terminal deoxynucleotidyl transferase-mediated deoxyuridine triphosphate-nick end labelling assay was used to measure hepatocyte apoptosis; G and N: Western blotting was used to detect the protein levels of uridine diphosphate glucuronosyltransferase 1A1 and cleaved caspase-3; H and O: Western blotting was used to detect the protein levels of phosphorylated mixed lineage kinase domain-like pseudokinase. $^{b}P < 0.01$ *vs* the control sgRNA or control group; $^{d}P < 0.01$ *vs* the carbon tetrachloride group. UGT1A1: Uridine diphosphate glucuronosyltransferase 1A1; ALT: Alanine transaminase; TBil: Total bilirubin; IBil: Indirect bilirubin; H&E: Hematoxylin and eosin; TUNEL: Transferase-mediated deoxyuridine triphosphate-nick end labelling; p-MLKL: Phosphorylated mixed lineage kinase domain-like pseudokinase; CCl_4: Carbon tetrachloride; KO: Knockout; GAPDH: Glyceraldehyde 3 phosphate dehydrogenase.

transcription of genes involved in fatty acid and TG synthesis, and plays an important role in the regulation of hepatic fatty acid metabolism[83,84]. ACSL4 is a member of the acyl-CoA synthetase family and promotes lipid peroxidation. Cells lacking ACSL4 resist lipid peroxidation by modifying their cellular lipid composition[85]. Inhibiting the expression of ACSL4 promotes mitochondrial respiration, enhancing the ability of liver cells to undergo fatty acid β-oxidation and reducing hepatic lipid accumulation[86]. Disturbances in hepatic lipid metabolism are closely associated with liver injury [87]. The accumulation of hepatic TGs can also increase ROS production, leading to an augmented oxidative stress response in liver cells[80]. In the context of liver injury, ER stress and oxidative stress interact with each other, creating a vicious cycle that facilitates the progression of liver injury[88]. In this study, we demonstrated through an animal model of fatty liver that alterations in hepatic lipid composition can lead to worsening liver damage. After *Ugt1a1* KO in the mouse liver, we observed an increased mortality rate in the *Ugt1a1*-KO group. This was accompanied by an intensification of ER stress and oxidative stress in the liver cells, resulting in heightened liver-cell apoptosis and programmed necrosis. These changes promoted the progression of liver fibrosis. This was demonstrated by an increase in the MDA content in the liver as well as elevated levels of GRP78, UCP2, cleaved caspase-3, and p-MLKL proteins. Furthermore, the lipid composition of the liver underwent changes, which were characterized by elevated levels of liver TC and TGs, reduced expression of MTP, and heightened expressions of SREBP1c and ACSL4. These alterations present barriers to lipid excretion, and promote increased lipid synthesis and lipid peroxidation. This suggests that *Ugt1a1* KO impacts the progression of liver injury by influencing ER stress and oxidative stress, while also exacerbating lipid metabolism disorder. These findings suggest that low levels of UGT1A1 may directly or indirectly contribute to the accumulation of lipids in the liver, delay recovery from liver injury, and promote the progression of liver damage. Thus, lipid metabolism disorder may be another mechanism by which UGT1A1 deficiency promotes the progression of liver damage.

ER stress, oxidative stress, and lipid metabolism disorders are closely linked to hepatocyte apoptosis and necroptosis. Reduced activity and low levels of UGT1A1 exacerbate ER stress, oxidative stress, and lipid metabolism disorders, thereby worsening liver-cell damage and promoting the progression of liver injury (Figure 9). Thus, low UGT1A1 levels may be one of the reasons for the progression of liver injury. Considering that UCB has an antioxidant effect in mild liver injury, these changes may be beneficial. However, high levels of IBil alone can also cause damage to hepatocyte mitochondria, leading to the production of ROS. Furthermore, decreased UGT1A1 activity can hinder the liver's capacity

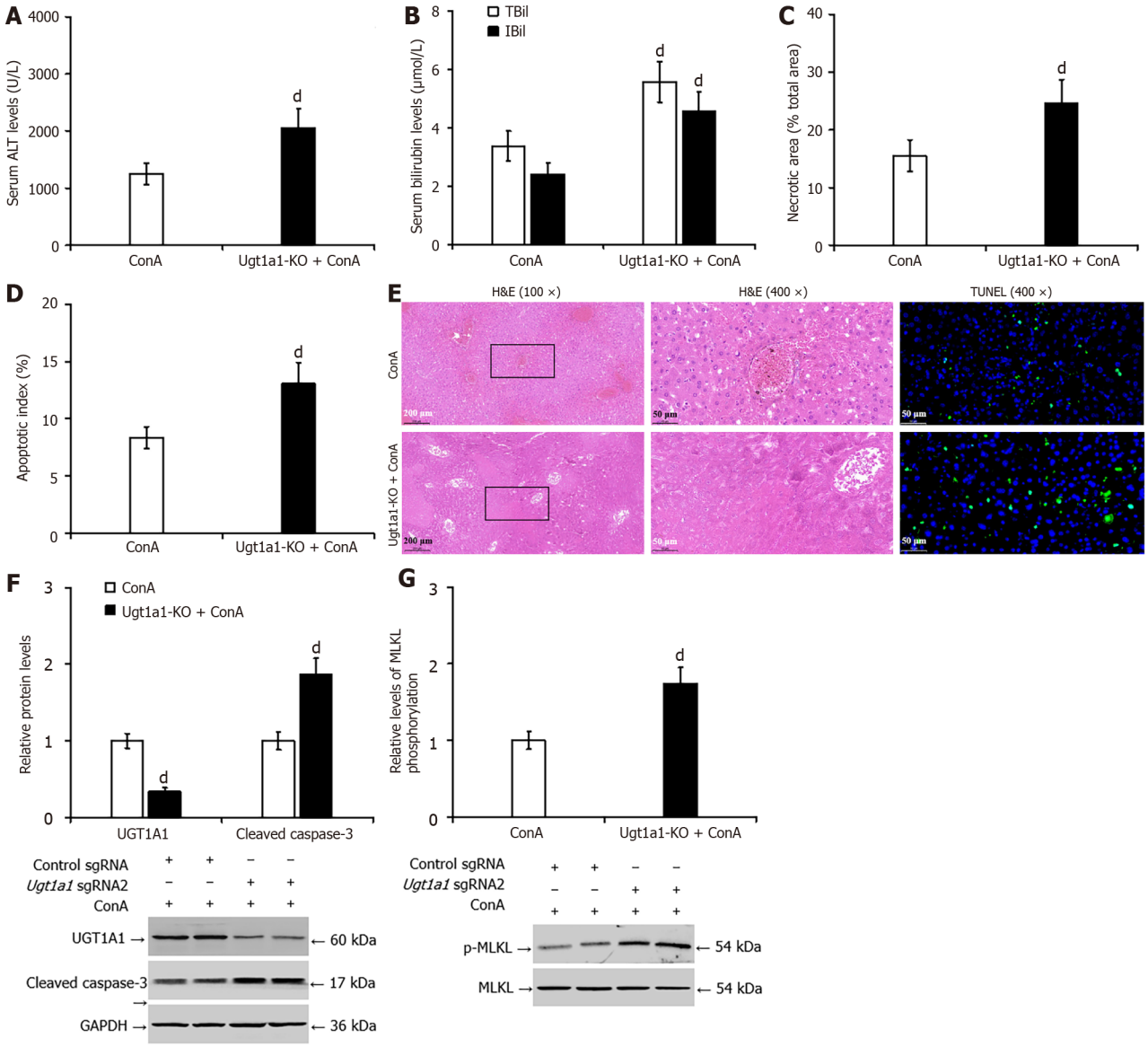

Figure 7 Knocking out uridine diphosphate glucuronosyltransferase 1A1 worsened concanavalin A-induced liver injury in mice. A: The enzyme rate method was used to detect the serum level of alanine transaminase in mice; B: The diazo method was used to detect the serum level of total bilirubin and indirect bilirubin; C and E: Pathological analysis of liver tissue by hematoxylin and eosin staining; D and E: The terminal deoxynucleotidyl transferase-mediated deoxyuridine triphosphate-nick end labelling assay was used to measure hepatocyte apoptosis; F: Western blotting was used to detect the protein levels of uridine diphosphate glucuronosyltransferase 1A1 and cleaved caspase-3; G: Western blotting was used to detect the protein levels of phosphorylated mixed lineage kinase domain-like pseudokinase. $^{d}P < 0.01$ *vs* the concanavalin A group. UGT1A1: Uridine diphosphate glucuronosyltransferase 1A1; ALT: Alanine transaminase; TBil: Total bilirubin; IBil: Indirect bilirubin; H&E: Hematoxylin and eosin; TUNEL: Transferase-mediated deoxyuridine triphosphate-nick end labelling; p-MLKL: Phosphorylated mixed lineage kinase domain-like pseudokinase; CCl_4: Carbon tetrachloride; KO: Knockout; GAPDH: Glyceraldehyde 3 phosphate dehydrogenase.

to metabolize other substances, leading to their accumulation in the liver. In severe liver injury, the excessive accumulation of such substances can have profoundly detrimental effects.

The shortcomings of this study should be acknowledged. The *Ugt1a1* gene was not completely knocked out, which may be related to the fact that the virus did not transfect all the hepatocytes. This research primarily focused on the subcellular level, and did not thoroughly investigate the specific regulatory mechanisms.

CONCLUSION

In liver injury, UGT1A1 expression is upregulated, and interference with this upregulation process may aggravate liver damage. The mitigation of liver injury by UGT1A1 may involve the alleviation of hepatocyte apoptosis and necroptosis mediated by ER stress, oxidative stress, and lipid metabolism disorder.

Table 1 Sequences of single guide ribonucleic acids used in the mouse experiments

sgRNA	sgRNA sequence (5' to 3')
Ugt1a1 sgRNA1	CACTAACAGCCTCCCAGCGT
Ugt1a1 sgRNA2	CACTAACAGCCTCCCAGCGT
Ugt1a1 sgRNA3	GCTGCACAATGCCGAGTTTA
Control sgRNA	AATCAACCGTGATAGTCTCG

sgRNA: Single guide ribonucleic acid; *Ugt1a1*: Uridine diphosphate glucuronosyltransferase 1A1.

Table 2 Information about primary antibodies

Antibody	Source	Lot number	Manufacturer	Reactivity
GAPDH	Mouse mAb	sc-365062	Santa Cruz Biotechnology, Dallas, TX, United States	Mouse, human
Cleaved caspase-3	Rabbit mAb	9664	Cell Signaling Technology, Danvers, MA, United States	Mouse, human
GRP78	Rabbit mAb	ab108615	Abcam, Cambridge, MA, United States	Mouse, human
MTP	Mouse mAb	sc-515742	Santa Cruz Biotechnology, Dallas, TX, United States	Mouse, human
UCP2	Mouse mAb	sc-390189	Santa Cruz Biotechnology, Dallas, TX, United States	Mouse, human
p-MLKL	Rabbit mAb	37333S	Cell Signaling Technology, Danvers, MA, United States	Mouse, human
MCAD	Mouse mAb	sc-365109	Santa Cruz Biotechnology, Dallas, TX, United States	Mouse, human
MLKL	Rabbit mAb	PA5-34733	Thermo Fisher Scientific, Waltham, MA, United States	Mouse, human
SREBP1c	Mouse mAb	MA5-16124	Thermo Fisher Scientific, Waltham, MA, United States	Mouse, human
ACSL4	Mouse mAb	sc-365230	Santa Cruz Biotechnology, Dallas, TX, United States	Mouse, human

ACSL4: Acyl-CoA synthetase long chain family member 4; GAPDH: Glyceraldehyde 3 phosphate dehydrogenase; GRP78: 78-kDa glucose-regulated protein; MTP: Microsomal triglyceride transfer protein; MCAD: Medium chain acyl-CoA dehydrogenase; MLKL: Mixed lineage kinase domain-like pseudokinase; SREBP1c: Cleaved sterol regulatory element-binding protein 1; UCP2: Uncoupling protein-2; p-MLKL: Phosphorylated mixed lineage kinase domain-like pseudokinase; mAb: Monoclonal antibody.

Table 3 Markers of liver function in patients with *uridine diphosphate glucuronosyltransferase 1A1* gene mutations

Patient	Gender	Age	ALT, U/L	AST, U/L	TBil, μmol/L	DBil, μmol/L	IBil, μmol/L	TBA, U/L
			Ref: 0-40	Ref: 0-34	Ref: 5.1-19.0	Ref: 1.7-6.8	Ref: 1.7-13.2	Ref: 0-50
1	Male	34	76↑	323↑	565.4↑	269.3↑	296.1↑	225.10↑
2	Male	43	26	28	184.2↑	24.8↑	155.8↑	160.00↑
3	Male	54	289↑	134↑	78.4↑	23.5↑	54.9↑	48.40↑
4	Female	25	22	28	368.7↑	186.6↑	182.1↑	242.54↑
5	Female	27	6	13	43.3↑	7.5↑	35.8↑	43.33↑
6	Male	21	6	15	50.2↑	10.0↑	40.2↑	38.93↑
7	Female	48	34	39↑	42.2↑	7.2↑	34.8↑	14.94↑

ALT: Alanine transaminase; AST: Aspartate aminotransferase; DBil: Direct bilirubin; IBil: Indirect bilirubin; TBil: Total bilirubin; TBA: Total bile acids.

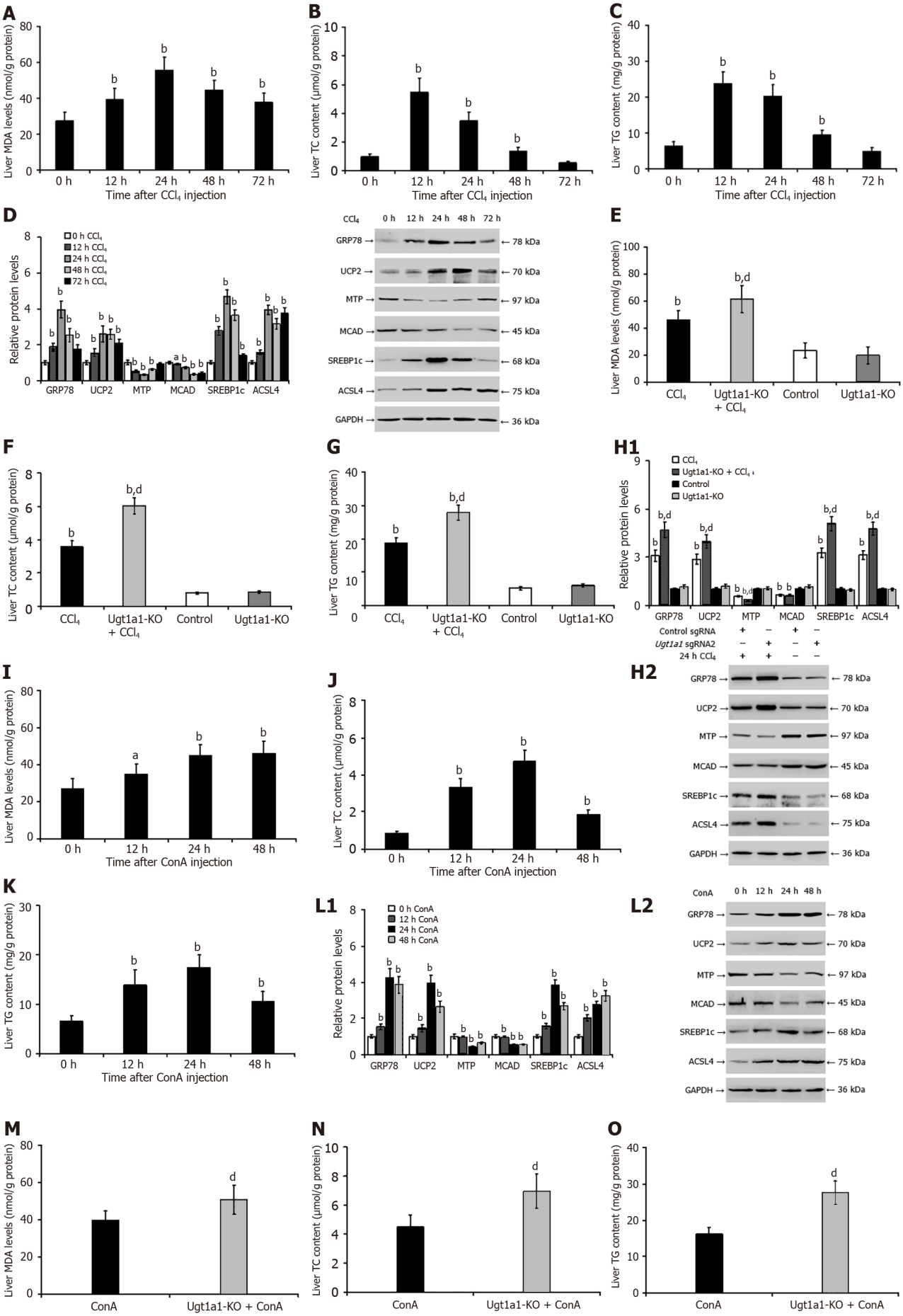
A
Liver MDA levels (nmol/g protein)
Time after CCl4 injection
0 h
12 h
24 h
48 h
72 h
B
Liver TC content (μmol/g protein)
C
Liver TG content (mg/g protein)
D
Relative protein levels
0 h CCl4
12 h CCl4
24 h CCl4
48 h CCl4
72 h CCl4
GRP78
UCP2
MTP
MCAD
SREBP1c
ACSL4
GAPDH
78 kDa
70 kDa
97 kDa
45 kDa
68 kDa
75 kDa
36 kDa
E
CCl4
Ugt1a1-KO + CCl4
Control
Ugt1a1-KO
F
G
H1
H2
Control sgRNA
Ugt1a1 sgRNA2
24 h CCl4
I
Time after ConA injection
J
K
L1
L2
ConA
M
N
O
ConA
Ugt1a1-KO + ConA

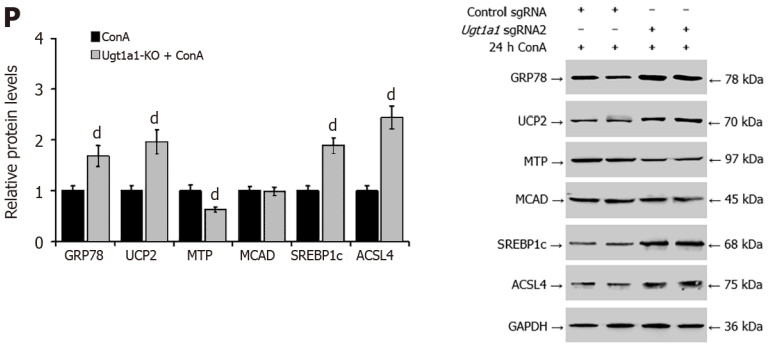

Figure 8 Interference with upregulation of uridine diphosphate glucuronosyltransferase 1A1 exacerbates hepatic endoplasmic reticulum stress, oxidative stress, and lipid metabolism disorder during liver injury. A-C: Malondialdehyde (MDA), triglyceride (TG), and total cholesterol (TC) contents in the livers of mice with carbon tetrachloride (CCl_4)-mediated liver injury; D: Related protein expressions in mice with CCl_4-mediated liver injury; E-G: MDA, TG, and TC contents in the livers of mice were measured in the *Ugt1a1* knockout model after treatment with CCl_4; H: Related protein expressions in CCl_4- mediated model mice with *Ugt1a1* knockout; I-K: MDA, TG, and TC contents in the livers of mice with concanavalin A (ConA)-mediated liver injury; L: Related protein expressions in mice with ConA-mediated liver injury; M-O: MDA, TG, and TC contents in the livers of mice were measured in the *Ugt1a1* knockout model after treatment with CCl_4; P: Related protein expressions in ConA-mediated model mice with *Ugt1a1* knockout. $^aP < 0.05$, $^bP < 0.01$ *vs* the 0 h or control group; $^dP < 0.01$ *vs* the CCl_4 groups or ConA groups. MDA: Malondialdehyde; TG: Triglyceride; TC: Total cholesterol; UGT1A1: Uridine diphosphate glucuronosyltransferase 1A1; MTP: Microsomal triglyceride transfer protein; MCAD: Medium-chain acyl-CoA dehydrogenase; SREBP1c: Cleaved sterol regulatory element-binding protein 1; ACSL4: Acyl-CoA synthetase long chain family member 4; GRP78: 78-kDa glucose-regulated protein; UCP2: Uncoupling protein-2; CCl_4: Carbon tetrachloride; ConA: Concanavalin A; KO: Knockout; GAPDH: Glyceraldehyde 3 phosphate dehydrogenase.

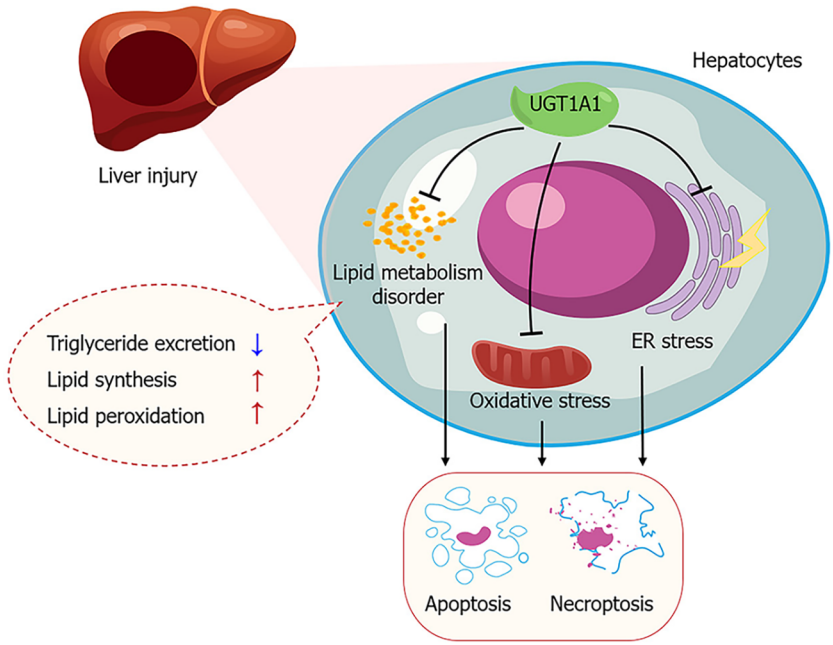

Figure 9 Uridine diphosphate glucuronosyltransferase 1A1 influences the mechanism of liver injury progression. The reduced activity and low levels of uridine diphosphate glucuronosyltransferase 1A1 exacerbate endoplasmic reticulum stress, oxidative stress, and disruptions in lipid metabolism, thereby increasing hepatocyte apoptosis and necroptosis, and promoting the progression of liver injury. UGT1A1: Uridine diphosphate glucuronosyltransferase 1A1; ER: Endoplasmic reticulum.

ARTICLE HIGHLIGHTS

Research background

Uridine diphosphate glucuronosyltransferase 1A1 (UGT1A1) is a member of the phase II metabolic enzyme family, which plays a significant role in metabolizing and detoxifying endogenous and exogenous substances. However, the role of UGT1A1 in liver disease remains controversial.

Research motivation

To determine the role and mechanism of UGT1A1 in the progression of liver injury.

Research objectives
To confirm that UGT1A1 prevents the progression of liver injury, and then elucidates the mechanism by which UGT1A1 delays the progression of liver damage from the viewpoints of endoplasmic reticulum (ER) stress, oxidative stress, and lipid metabolism disorder.

Research methods
We investigated the relationship between UGT1A1 expression and liver injury through clinical research. Additionally, the impact and mechanism of UGT1A1 on the progression of liver injury was analyzed through a mouse model study.

Research results
The expression of UGT1A1 in hepatocytes was upregulated as a compensatory response during liver injury. The upregulation of UGT1A1 was beneficial for hepatocytes to avoid apoptosis and necroptosis under conditions of ER stress, oxidative stress, and disrupted lipid metabolism. Disruption of this compensatory upregulation of UGT1A1 during liver injury could potentially expedite the progression of liver damage.

Research conclusions
UGT1A1 prevents the progression of liver injury by reducing hepatocyte apoptosis and necroptosis mediated by ER stress, oxidative stress, and lipid metabolism disorder.

Research perspectives
This study highlights the role of UGT1A1 in preventing the progression of liver injury. Further investigation is required to understand the specific mechanisms by which UGT1A1 regulates ER stress, oxidative stress, especially lipid metabolism, to hinder the progression of liver injury. The research findings enrich the understanding of the mechanism of liver injury progression and provide potential intervention targets for the treatment of liver injury.

FOOTNOTES

Co-first authors: Jin-Lian Jiang and Yi-Yang Zhou.

Author contributions: Jiang JL and Zhou YY contributed equally to this work; Jiang JL, Zhou YY, and He YH conceived and designed the research; Jiang JL, Zhou YY, Zhong WW, Luo LY, Liu SY, and Xie XY collected data and conducted research; Jiang JL, Zhou YY, Mu MY, Jiang ZG, Xue Y, and Zhang J analyzed and interpreted data; Jiang JL and Zhou YY wrote the initial draft; He YH revised the manuscript; and all authors read and approved the final version of the manuscript.

Supported by the Science and Technology Research Foundations of Guizhou Province, No. QKHJC-ZK(2022)YB642; Zunyi Science and Technology Plan Project, No. ZSKHHZ(2022)344, No. ZSKHHZ(2022)360, and No. ZYK160; Hubei Province Central Leading Local Science and Technology Development Special Project, No. 2022BCE030; Changzhou Science and Technology Projects, No. CE20225054; and Bijie City Science and Planning Bureau, No. BKH(2022)8.

Institutional review board statement: The study was reviewed and approved by the Zunyi Medical University Medical Ethics Review Committee [Approval No. ZYFYLS (2018)28 and No. ZYLS(2022)1-059].

Institutional animal care and use committee statement: All procedures involving animals were reviewed and approved by the Affidavit of Approval of Animal Welfare and Ethical of Zunyi Medical University (Approval No. ZMU21-2107-003 and No. ZMU11-2203-314).

Conflict-of-interest statement: The authors declare that they have no conflict of interest.

Data sharing statement: The datasets generated and analyzed during the current study are available from the corresponding author on reasonable request.

ARRIVE guidelines statement: The authors have read the ARRIVE guidelines, and the manuscript was prepared and revised according to the ARRIVE guidelines.

Country/Territory of origin: China

ORCID number: Jin-Lian Jiang 0000-0002-0791-9680; Yi-Yang Zhou 0000-0002-1549-1821; Wei-Wei Zhong 0000-0002-9736-8148; Lin-Yan Luo 0009-0003-8729-3060; Si-Ying Liu 0000-0001-9938-4232; Xiao-Yu Xie 0009-0001-5083-3073; Mao-Yuan Mu 0000-0001-5632-0167; Zhi-Gang Jiang 0000-0003-4539-6988; Yuan Xue 0000-0002-5428-0058; Jian Zhang 0009-0001-7312-2725; Yi-Huai He 0000-0002-8639-3436.

S-Editor: Chen YL

L-Editor: A
P-Editor: Yu HG

REFERENCES

1 **Mano ECC**, Scott AL, Honorio KM. UDP-glucuronosyltransferases: Structure, Function and Drug Design Studies. *Curr Med Chem* 2018; **25**: 3247-3255 [PMID: 29484974 DOI: 10.2174/0929867325666180226111311]
2 **Zhan Z**, Dai F, Zhang T, Chen Y, She J, Jiang H, Liu S, Gu T, Tang L. Oridonin alleviates hyperbilirubinemia through activating LXRα-UGT1A1 axis. *Pharmacol Res* 2022; **178**: 106188 [PMID: 35338002 DOI: 10.1016/j.phrs.2022.106188]
3 **Vitek L**, Hinds TD Jr, Stec DE, Tiribelli C. The physiology of bilirubin: health and disease equilibrium. *Trends Mol Med* 2023; **29**: 315-328 [PMID: 36828710 DOI: 10.1016/j.molmed.2023.01.007]
4 **Liu D**, Yu Q, Ning Q, Liu Z, Song J. The relationship between UGT1A1 gene & various diseases and prevention strategies. *Drug Metab Rev* 2022; **54**: 1-21 [PMID: 34807779 DOI: 10.1080/03602532.2021.2001493]
5 **Longhi MS**, Vuerich M, Kalbasi A, Kenison JE, Yeste A, Csizmadia E, Vaughn B, Feldbrugge L, Mitsuhashi S, Wegiel B, Otterbein L, Moss A, Quintana FJ, Robson SC. Bilirubin suppresses Th17 immunity in colitis by upregulating CD39. *JCI Insight* 2017; **2** [PMID: 28469075 DOI: 10.1172/jci.insight.92791]
6 **Hamoud AR**, Weaver L, Stec DE, Hinds TD Jr. Bilirubin in the Liver-Gut Signaling Axis. *Trends Endocrinol Metab* 2018; **29**: 140-150 [PMID: 29409713 DOI: 10.1016/j.tem.2018.01.002]
7 **Bates EA**, Kipp ZA, Martinez GJ, Badmus OO, Soundarapandian MM, Foster D, Xu M, Creeden JF, Greer JR, Morris AJ, Stec DE, Hinds TD Jr. Suppressing Hepatic UGT1A1 Increases Plasma Bilirubin, Lowers Plasma Urobilin, Reorganizes Kinase Signaling Pathways and Lipid Species and Improves Fatty Liver Disease. *Biomolecules* 2023; **13** [PMID: 36830621 DOI: 10.3390/biom13020252]
8 **Lei HP**, Qin M, Cai LY, Wu H, Tang L, Liu JE, Deng CY, Liu YB, Zhu Q, Li HP, Hu W, Yang M, Zhu YZ, Zhong SL. UGT1A1 rs4148323 A Allele is Associated With Increased 2-Hydroxy Atorvastatin Formation and Higher Death Risk in Chinese Patients With Coronary Artery Disease. *Front Pharmacol* 2021; **12**: 586973 [PMID: 33762934 DOI: 10.3389/fphar.2021.586973]
9 **Strassburg CP**. Hyperbilirubinemia syndromes (Gilbert-Meulengracht, Crigler-Najjar, Dubin-Johnson, and Rotor syndrome). *Best Pract Res Clin Gastroenterol* 2010; **24**: 555-571 [PMID: 20955959 DOI: 10.1016/j.bpg.2010.07.007]
10 **Qian S**, Kumar P, Testai FD. Bilirubin Encephalopathy. *Curr Neurol Neurosci Rep* 2022; **22**: 343-353 [PMID: 35588044 DOI: 10.1007/s11910-022-01204-8]
11 **Veel T**, Villanger O, Holthe MR, Skjørten FS, Raeder MG. Intravenous bilirubin infusion causes vacuolization of the cytoplasm of hepatocytes and canalicular cholestasis. *Acta Physiol Scand* 1991; **143**: 421-429 [PMID: 1815476 DOI: 10.1111/j.1748-1716.1991.tb09254.x]
12 **Laskar AA**, Khan MA, Rahmani AH, Fatima S, Younus H. Thymoquinone, an active constituent of Nigella sativa seeds, binds with bilirubin and protects mice from hyperbilirubinemia and cyclophosphamide-induced hepatotoxicity. *Biochimie* 2016; **127**: 205-213 [PMID: 27265787 DOI: 10.1016/j.biochi.2016.05.020]
13 **Liu D**, Yu Q, Li Z, Zhang L, Hu M, Wang C, Liu Z. UGT1A1 dysfunction increases liver burden and aggravates hepatocyte damage caused by long-term bilirubin metabolism disorder. *Biochem Pharmacol* 2021; **190**: 114592 [PMID: 33961837 DOI: 10.1016/j.bcp.2021.114592]
14 **Goon CP**, Wang LZ, Wong FC, Thuya WL, Ho PC, Goh BC. UGT1A1 Mediated Drug Interactions and its Clinical Relevance. *Curr Drug Metab* 2016; **17**: 100-106 [PMID: 26526830 DOI: 10.2174/1389200216666151103121253]
15 **Takano M**, Sugiyama T. UGT1A1 polymorphisms in cancer: impact on irinotecan treatment. *Pharmgenomics Pers Med* 2017; **10**: 61-68 [PMID: 28280378 DOI: 10.2147/PGPM.S108656]
16 **Hahn RZ**, Antunes MV, Verza SG, Perassolo MS, Suyenaga ES, Schwartsmann G, Linden R. Pharmacokinetic and Pharmacogenetic Markers of Irinotecan Toxicity. *Curr Med Chem* 2019; **26**: 2085-2107 [PMID: 29932028 DOI: 10.2174/0929867325666180622141101]
17 **McGill MR**, Jaeschke H. Metabolism and disposition of acetaminophen: recent advances in relation to hepatotoxicity and diagnosis. *Pharm Res* 2013; **30**: 2174-2187 [PMID: 23462933 DOI: 10.1007/s11095-013-1007-6]
18 **Chang JC**, Liu EH, Lee CN, Lin YC, Yu MC, Bai KJ, Chen HY. UGT1A1 polymorphisms associated with risk of induced liver disorders by anti-tuberculosis medications. *Int J Tuberc Lung Dis* 2012; **16**: 376-378 [PMID: 22230213 DOI: 10.5588/ijtld.11.0404]
19 **Henriksen JN**, Bøttger P, Hermansen CK, Ladefoged SA, Nissen PH, Hamilton-Dutoit S, Fink TL, Donskov F. Pazopanib-Induced Liver Toxicity in Patients With Metastatic Renal Cell Carcinoma: Effect of UGT1A1 Polymorphism on Pazopanib Dose Reduction, Safety, and Patient Outcomes. *Clin Genitourin Cancer* 2020; **18**: 62-68.e2 [PMID: 31640912 DOI: 10.1016/j.clgc.2019.09.013]
20 **Korprasertthaworn P**, Chau N, Nair PC, Rowland A, Miners JO. Inhibition of human UDP-glucuronosyltransferase (UGT) enzymes by kinase inhibitors: Effects of dabrafenib, ibrutinib, nintedanib, trametinib and BIBF 1202. *Biochem Pharmacol* 2019; **169**: 113616 [PMID: 31445021 DOI: 10.1016/j.bcp.2019.08.018]
21 **Jiang JL**, Liu X, Pan ZQ, Jiang XL, Shi JH, Chen Y, Yi Y, Zhong WW, Liu KY, He YH. Postoperative jaundice related to UGT1A1 and ABCB11 gene mutations: A case report and literature review. *World J Clin Cases* 2023; **11**: 1393-1402 [PMID: 36926131 DOI: 10.12998/wjcc.v11.i6.1393]
22 **Yuan L**, Zeng BM, Liu LL, Ren Y, Yang YQ, Chu J, Li Y, Yang FW, He YH, Lin SD. Risk factors for progression to acute-on-chronic liver failure during severe acute exacerbation of chronic hepatitis B virus infection. *World J Gastroenterol* 2019; **25**: 2327-2337 [PMID: 31148904 DOI: 10.3748/wjg.v25.i19.2327]
23 **Ferstl P**, Trebicka J. Acute Decompensation and Acute-on-Chronic Liver Failure. *Clin Liver Dis* 2021; **25**: 419-430 [PMID: 33838858 DOI: 10.1016/j.cld.2021.01.009]
24 **Chen EQ**, Zeng F, Zhou LY, Tang H. Early warning and clinical outcome prediction of acute-on-chronic hepatitis B liver failure. *World J Gastroenterol* 2015; **21**: 11964-11973 [PMID: 26576085 DOI: 10.3748/wjg.v21.i42.11964]
25 **Cui S**, Li Y, Zhang X, Wu B, Li M, Gao J, Xu L, Xia H. Fibroblast growth factor 5 overexpression ameliorated lipopolysaccharide-induced apoptosis of hepatocytes through regulation of the phosphoinositide-3-kinase/protein kinase B pathway. *Chin Med J (Engl)* 2022; **135**: 2859-2868 [PMID: 36728504 DOI: 10.1097/CM9.0000000000002540]
26 **Xu Q**, Guo J, Li X, Wang Y, Wang D, Xiao K, Zhu H, Wang X, Hu CA, Zhang G, Liu Y. Necroptosis Underlies Hepatic Damage in a Piglet Model of Lipopolysaccharide-Induced Sepsis. *Front Immunol* 2021; **12**: 633830 [PMID: 33777021 DOI: 10.3389/fimmu.2021.633830]

27 **Yuan Z**, Zhang H, Hasnat M, Ding J, Chen X, Liang P, Sun L, Zhang L, Jiang Z. A new perspective of triptolide-associated hepatotoxicity: Liver hypersensitivity upon LPS stimulation. *Toxicology* 2019; **414**: 45-56 [PMID: 30633930 DOI: 10.1016/j.tox.2019.01.005]

28 **Berthiaume F**, Barbe L, Mokuno Y, MacDonald AD, Jindal R, Yarmush ML. Steatosis reversibly increases hepatocyte sensitivity to hypoxia-reoxygenation injury. *J Surg Res* 2009; **152**: 54-60 [PMID: 18599084 DOI: 10.1016/j.jss.2007.12.784]

29 **Schwabe RF**, Luedde T. Apoptosis and necroptosis in the liver: a matter of life and death. *Nat Rev Gastroenterol Hepatol* 2018; **15**: 738-752 [PMID: 30250076 DOI: 10.1038/s41575-018-0065-y]

30 **Liu J**, Wu F, Wang M, Tao M, Liu Z, Hai Z. Caspase-3-Responsive Fluorescent/Photoacoustic Imaging of Tumor Apoptosis. *Anal Chem* 2023; **95**: 9404-9408 [PMID: 37306631 DOI: 10.1021/acs.analchem.3c01387]

31 **Fauster A**, Rebsamen M, Willmann KL, César-Razquin A, Girardi E, Bigenzahn JW, Schischlik F, Scorzoni S, Bruckner M, Konecka J, Hörmann K, Heinz LX, Boztug K, Superti-Furga G. Systematic genetic mapping of necroptosis identifies SLC39A7 as modulator of death receptor trafficking. *Cell Death Differ* 2019; **26**: 1138-1155 [PMID: 30237509 DOI: 10.1038/s41418-018-0192-6]

32 **Ajoolabady A**, Kaplowitz N, Lebeaupin C, Kroemer G, Kaufman RJ, Malhi H, Ren J. Endoplasmic reticulum stress in liver diseases. *Hepatology* 2023; **77**: 619-639 [PMID: 35524448 DOI: 10.1002/hep.32562]

33 **Dai C**, Xiao X, Li D, Tun S, Wang Y, Velkov T, Tang S. Chloroquine ameliorates carbon tetrachloride-induced acute liver injury in mice *via* the concomitant inhibition of inflammation and induction of apoptosis. *Cell Death Dis* 2018; **9**: 1164 [PMID: 30478280 DOI: 10.1038/s41419-018-1136-2]

34 **Heymann F**, Hamesch K, Weiskirchen R, Tacke F. The concanavalin A model of acute hepatitis in mice. *Lab Anim* 2015; **49**: 12-20 [PMID: 25835734 DOI: 10.1177/0023677215572841]

35 **Tuominen I**, Fuqua BK, Pan C, Renaud N, Wroblewski K, Civelek M, Clerkin K, Asaryan A, Haroutunian SG, Loureiro J, Borawski J, Roma G, Knehr J, Carbone W, French S, Parks BW, Hui ST, Mehrabian M, Magyar C, Cantor RM, Ukomadu C, Lusis AJ, Beaven SW. The Genetic Architecture of Carbon Tetrachloride-Induced Liver Fibrosis in Mice. *Cell Mol Gastroenterol Hepatol* 2021; **11**: 199-220 [PMID: 32866618 DOI: 10.1016/j.jcmgh.2020.08.010]

36 **Nautiyal N**, Maheshwari D, Tripathi DM, Kumar D, Kumari R, Gupta S, Sharma S, Mohanty S, Parasar A, Bihari C, Biswas S, Rastogi A, Maiwall R, Kumar A, Sarin SK. Establishment of a murine model of acute-on-chronic liver failure with multi-organ dysfunction. *Hepatol Int* 2021; **15**: 1389-1401 [PMID: 34435344 DOI: 10.1007/s12072-021-10244-0]

37 **Xiang X**, Feng D, Hwang S, Ren T, Wang X, Trojnar E, Matyas C, Mo R, Shang D, He Y, Seo W, Shah VH, Pacher P, Xie Q, Gao B. Interleukin-22 ameliorates acute-on-chronic liver failure by reprogramming impaired regeneration pathways in mice. *J Hepatol* 2020; **72**: 736-745 [PMID: 31786256 DOI: 10.1016/j.jhep.2019.11.013]

38 **Glibert B**, Bourleaux V, Peeters R, Reynolds T, Vranken G. Analytical Performance Verification of the Beckman Coulter AU5800 Clinical Chemistry Analyser Against Recognized Quality Specifications Reveals Relevance of Method Harmonization. *Clin Lab* 2016; **62**: 57-72 [PMID: 27012034 DOI: 10.7754/clin.lab.2015.150521]

39 **Hou Y**, Sun X, Gheinani PT, Guan X, Sharma S, Zhou Y, Jin C, Yang Z, Naren AP, Yin J, Denning TL, Gewirtz AT, Liu Y, Xie Z, Li C. Epithelial SMYD5 Exaggerates IBD by Down-regulating Mitochondrial Functions *via* Post-Translational Control of PGC-1α Stability. *Cell Mol Gastroenterol Hepatol* 2022; **14**: 375-403 [PMID: 35643234 DOI: 10.1016/j.jcmgh.2022.05.006]

40 **Bao W**, Li K, Rong S, Yao P, Hao L, Ying C, Zhang X, Nussler A, Liu L. Curcumin alleviates ethanol-induced hepatocytes oxidative damage involving heme oxygenase-1 induction. *J Ethnopharmacol* 2010; **128**: 549-553 [PMID: 20080166 DOI: 10.1016/j.jep.2010.01.029]

41 **Mi XX**, Yan J, Ma XJ, Zhu GL, Gao YD, Yang WJ, Kong XW, Chen GY, Shi JP, Gong L. Analysis of the UGT1A1 Genotype in Hyperbilirubinemia Patients: Differences in Allele Frequency and Distribution. *Biomed Res Int* 2019; **2019**: 6272174 [PMID: 31467903 DOI: 10.1155/2019/6272174]

42 **Gu L**, Han Y, Zhang D, Gong Q, Zhang X. Genetic testing of UGT1A1 in the diagnosis of Gilbert syndrome: The discovery of seven novel variants in the Chinese population. *Mol Genet Genomic Med* 2022; **10**: e1958 [PMID: 35426266 DOI: 10.1002/mgg3.1958]

43 **Fretzayas A**, Moustaki M, Liapi O, Karpathios T. Gilbert syndrome. *Eur J Pediatr* 2012; **171**: 11-15 [PMID: 22160004 DOI: 10.1007/s00431-011-1641-0]

44 **Radlović N**. Hereditary hyperbilirubinemias. *Srp Arh Celok Lek* 2014; **142**: 257-260 [PMID: 24839786 DOI: 10.2298/sarh1404257r]

45 **Strassburg CP**. Gilbert-Meulengracht's syndrome and pharmacogenetics: is jaundice just the tip of the iceberg? *Drug Metab Rev* 2010; **42**: 168-181 [PMID: 20070246 DOI: 10.3109/03602530903209429]

46 **Yang Y**, Zhou M, Hu M, Cui Y, Zhong Q, Liang L, Huang F. UGT1A1*6 and UGT1A1*28 polymorphisms are correlated with irinotecan-induced toxicity: A meta-analysis. *Asia Pac J Clin Oncol* 2018; **14**: e479-e489 [PMID: 29932297 DOI: 10.1111/ajco.13028]

47 **Teh LK**, Hashim H, Zakaria ZA, Salleh MZ. Polymorphisms of UGT1A1*6, UGT1A1*27 & UGT1A1*28 in three major ethnic groups from Malaysia. *Indian J Med Res* 2012; **136**: 249-259 [PMID: 22960892]

48 **Fevery J**. Bilirubin in clinical practice: a review. *Liver Int* 2008; **28**: 592-605 [PMID: 18433389 DOI: 10.1111/j.1478-3231.2008.01716.x]

49 **Rawat V**, Bortolussi G, Gazzin S, Tiribelli C, Muro AF. Bilirubin-Induced Oxidative Stress Leads to DNA Damage in the Cerebellum of Hyperbilirubinemic Neonatal Mice and Activates DNA Double-Strand Break Repair Pathways in Human Cells. *Oxid Med Cell Longev* 2018; **2018**: 1801243 [PMID: 30598724 DOI: 10.1155/2018/1801243]

50 **Zhang J**, Guo J, Yang N, Huang Y, Hu T, Rao C. Endoplasmic reticulum stress-mediated cell death in liver injury. *Cell Death Dis* 2022; **13**: 1051 [PMID: 36535923 DOI: 10.1038/s41419-022-05444-x]

51 **Li X**, Li X, Lu J, Huang Y, Lv L, Luan Y, Liu R, Sun R. Saikosaponins induced hepatotoxicity in mice *via* lipid metabolism dysregulation and oxidative stress: a proteomic study. *BMC Complement Altern Med* 2017; **17**: 219 [PMID: 28420359 DOI: 10.1186/s12906-017-1733-0]

52 **Lukas J**, Pospech J, Oppermann C, Hund C, Iwanov K, Pantoom S, Petters J, Frech M, Seemann S, Thiel FG, Modenbach JM, Bolsmann R, de Freitas Chama L, Kraatz F, El-Hage F, Gronbach M, Klein A, Müller R, Salloch S, Weiss FU, Simon P, Wagh P, Klemenz A, Krüger E, Mayerle J, Delcea M, Kragl U, Beller M, Rolfs A, Lerch MM, Sendler M. Role of endoplasmic reticulum stress and protein misfolding in disorders of the liver and pancreas. *Adv Med Sci* 2019; **64**: 315-323 [PMID: 30978662 DOI: 10.1016/j.advms.2019.03.004]

53 **Kapoor A**, Sanyal AJ. Endoplasmic reticulum stress and the unfolded protein response. *Clin Liver Dis* 2009; **13**: 581-590 [PMID: 19818306 DOI: 10.1016/j.cld.2009.07.004]

54 **Schmitz ML**, Shaban MS, Albert BV, Gökçen A, Kracht M. The Crosstalk of Endoplasmic Reticulum (ER) Stress Pathways with NF-κB: Complex Mechanisms Relevant for Cancer, Inflammation and Infection. *Biomedicines* 2018; **6** [PMID: 29772680 DOI: 10.3390/biomedicines6020058]

55 **Hu XW**, Li XM, Wang AM, Fu YM, Zhang FJ, Zeng F, Cao LP, Long H, Xiong YH, Xu J, Li J. Caffeine alleviates acute liver injury by

inducing the expression of NEDD4L and deceasing GRP78 level *via* ubiquitination. *Inflamm Res* 2022; **71**: 1213-1227 [PMID: 35802146 DOI: 10.1007/s00011-022-01603-0]

56 **Müllebner A**, Moldzio R, Redl H, Kozlov AV, Duvigneau JC. Heme Degradation by Heme Oxygenase Protects Mitochondria but Induces ER Stress *via* Formed Bilirubin. *Biomolecules* 2015; **5**: 679-701 [PMID: 25942605 DOI: 10.3390/biom5020679]

57 **Oakes GH**, Bend JR. Global changes in gene regulation demonstrate that unconjugated bilirubin is able to upregulate and activate select components of the endoplasmic reticulum stress response pathway. *J Biochem Mol Toxicol* 2010; **24**: 73-88 [PMID: 20196124 DOI: 10.1002/jbt.20313]

58 **Qaisiya M**, Brischetto C, Jašprová J, Vitek L, Tiribelli C, Bellarosa C. Bilirubin-induced ER stress contributes to the inflammatory response and apoptosis in neuronal cells. *Arch Toxicol* 2017; **91**: 1847-1858 [PMID: 27578021 DOI: 10.1007/s00204-016-1835-3]

59 **Schiavon E**, Smalley JL, Newton S, Greig NH, Forsythe ID. Neuroinflammation and ER-stress are key mechanisms of acute bilirubin toxicity and hearing loss in a mouse model. *PLoS One* 2018; **13**: e0201022 [PMID: 30106954 DOI: 10.1371/journal.pone.0201022]

60 **Tian RD**, Chen YQ, He YH, Tang YJ, Chen GM, Yang FW, Li Y, Huang WG, Chen H, Liu X, Lin SD. Phosphorylation of eIF2α mitigates endoplasmic reticulum stress and hepatocyte necroptosis in acute liver injury. *Ann Hepatol* 2020; **19**: 79-87 [PMID: 31548168 DOI: 10.1016/j.aohep.2019.05.008]

61 **Chen YF**, Liu SY, Cheng QJ, Wang YJ, Chen S, Zhou YY, Liu X, Jiang ZG, Zhong WW, He YH. Intracellular alpha-fetoprotein mitigates hepatocyte apoptosis and necroptosis by inhibiting endoplasmic reticulum stress. *World J Gastroenterol* 2022; **28**: 3201-3217 [PMID: 36051342 DOI: 10.3748/wjg.v28.i26.3201]

62 **Cichoż-Lach H**, Michalak A. Oxidative stress as a crucial factor in liver diseases. *World J Gastroenterol* 2014; **20**: 8082-8091 [PMID: 25009380 DOI: 10.3748/wjg.v20.i25.8082]

63 **Sinha N**, Dabla PK. Oxidative stress and antioxidants in hypertension-a current review. *Curr Hypertens Rev* 2015; **11**: 132-142 [PMID: 26022210 DOI: 10.2174/1573402111666150529130922]

64 **Ming S**, Tian J, Ma K, Pei C, Li L, Wang Z, Fang Z, Liu M, Dong H, Li W, Zeng J, Peng Y, Gao X. Oxalate-induced apoptosis through ERS-ROS-NF-κB signalling pathway in renal tubular epithelial cell. *Mol Med* 2022; **28**: 88 [PMID: 35922749 DOI: 10.1186/s10020-022-00494-5]

65 **Wang J**, He W, Tsai PJ, Chen PH, Ye M, Guo J, Su Z. Mutual interaction between endoplasmic reticulum and mitochondria in nonalcoholic fatty liver disease. *Lipids Health Dis* 2020; **19**: 72 [PMID: 32284046 DOI: 10.1186/s12944-020-01210-0]

66 **Luby A**, Alves-Guerra MC. UCP2 as a Cancer Target through Energy Metabolism and Oxidative Stress Control. *Int J Mol Sci* 2022; **23** [PMID: 36499405 DOI: 10.3390/ijms232315077]

67 **Seubert JM**, Darmon AJ, El-Kadi AO, D'Souza SJ, Bend JR. Apoptosis in murine hepatoma hepa 1c1c7 wild-type, C12, and C4 cells mediated by bilirubin. *Mol Pharmacol* 2002; **62**: 257-264 [PMID: 12130676 DOI: 10.1124/mol.62.2.257]

68 **Oakes GH**, Bend JR. Early steps in bilirubin-mediated apoptosis in murine hepatoma (Hepa 1c1c7) cells are characterized by aryl hydrocarbon receptor-independent oxidative stress and activation of the mitochondrial pathway. *J Biochem Mol Toxicol* 2005; **19**: 244-255 [PMID: 16173058 DOI: 10.1002/jbt.20086]

69 **Keshavan P**, Schwemberger SJ, Smith DL, Babcock GF, Zucker SD. Unconjugated bilirubin induces apoptosis in colon cancer cells by triggering mitochondrial depolarization. *Int J Cancer* 2004; **112**: 433-445 [PMID: 15382069 DOI: 10.1002/ijc.20418]

70 **Bortolussi G**, Codarin E, Antoniali G, Vascotto C, Vodret S, Arena S, Cesaratto L, Scaloni A, Tell G, Muro AF. Impairment of enzymatic antioxidant defenses is associated with bilirubin-induced neuronal cell death in the cerebellum of Ugt1 KO mice. *Cell Death Dis* 2015; **6**: e1739 [PMID: 25950469 DOI: 10.1038/cddis.2015.113]

71 **Daood MJ**, Hoyson M, Watchko JF. Lipid peroxidation is not the primary mechanism of bilirubin-induced neurologic dysfunction in jaundiced Gunn rat pups. *Pediatr Res* 2012; **72**: 455-459 [PMID: 22902434 DOI: 10.1038/pr.2012.111]

72 **You L**, Zhao Y, Kuca K, Wang X, Oleksak P, Chrienova Z, Nepovimova E, Jaćević V, Wu Q, Wu W. Hypoxia, oxidative stress, and immune evasion: a trinity of the trichothecenes T-2 toxin and deoxynivalenol (DON). *Arch Toxicol* 2021; **95**: 1899-1915 [PMID: 33765170 DOI: 10.1007/s00204-021-03030-2]

73 **Wang Y**, Liu X, Jing H, Ren H, Xu S, Guo M. Trimethyltin induces apoptosis and necroptosis of mouse liver by oxidative stress through YAP phosphorylation. *Ecotoxicol Environ Saf* 2022; **248**: 114327 [PMID: 36434999 DOI: 10.1016/j.ecoenv.2022.114327]

74 **Turgeon D**, Chouinard S, Belanger P, Picard S, Labbe JF, Borgeat P, Belanger A. Glucuronidation of arachidonic and linoleic acid metabolites by human UDP-glucuronosyltransferases. *J Lipid Res* 2003; **44**: 1182-1191 [PMID: 12639971 DOI: 10.1194/jlr.M300010-JLR200]

75 **Moncan M**, Mnich K, Blomme A, Almanza A, Samali A, Gorman AM. Regulation of lipid metabolism by the unfolded protein response. *J Cell Mol Med* 2021; **25**: 1359-1370 [PMID: 33398919 DOI: 10.1111/jcmm.16255]

76 **Liu C**, Zhou B, Meng M, Zhao W, Wang D, Yuan Y, Zheng Y, Qiu J, Li Y, Li G, Xiong X, Bian H, Zhang H, Wang H, Ma X, Hu C, Xu L, Lu Y. FOXA3 induction under endoplasmic reticulum stress contributes to non-alcoholic fatty liver disease. *J Hepatol* 2021; **75**: 150-162 [PMID: 33548387 DOI: 10.1016/j.jhep.2021.01.042]

77 **Luo Y**, Jiao Q, Chen Y. Targeting endoplasmic reticulum stress-the responder to lipotoxicity and modulator of non-alcoholic fatty liver diseases. *Expert Opin Ther Targets* 2022; **26**: 1073-1085 [PMID: 36657744 DOI: 10.1080/14728222.2022.2170780]

78 **Li J**, Li X, Liu D, Zhang S, Tan N, Yokota H, Zhang P. Phosphorylation of eIF2α signaling pathway attenuates obesity-induced non-alcoholic fatty liver disease in an ER stress and autophagy-dependent manner. *Cell Death Dis* 2020; **11**: 1069 [PMID: 33318479 DOI: 10.1038/s41419-020-03264-5]

79 **Hussain MM**, Shi J, Dreizen P. Microsomal triglyceride transfer protein and its role in apoB-lipoprotein assembly. *J Lipid Res* 2003; **44**: 22-32 [PMID: 12518019 DOI: 10.1194/jlr.r200014-jlr200]

80 **Vuorio A**, Tikkanen MJ, Kovanen PT. Inhibition of hepatic microsomal triglyceride transfer protein - a novel therapeutic option for treatment of homozygous familial hypercholesterolemia. *Vasc Health Risk Manag* 2014; **10**: 263-270 [PMID: 24851052 DOI: 10.2147/VHRM.S36641]

81 **Ibrahim SA**, Temtem T. Medium-Chain Acyl-CoA Dehydrogenase Deficiency. 2023 Jul 10. In: StatPearls [Internet]. Treasure Island (FL): StatPearls Publishing; 2024 Jan- [PMID: 32809672]

82 **Mason E**, Hindmarch CCT, Dunham-Snary KJ. Medium-chain Acyl-COA dehydrogenase deficiency: Pathogenesis, diagnosis, and treatment. *Endocrinol Diabetes Metab* 2023; **6**: e385 [PMID: 36300606 DOI: 10.1002/edm2.385]

83 **Jang H**, Lee GY, Selby CP, Lee G, Jeon YG, Lee JH, Cheng KK, Titchenell P, Birnbaum MJ, Xu A, Sancar A, Kim JB. SREBP1c-CRY1 signalling represses hepatic glucose production by promoting FOXO1 degradation during refeeding. *Nat Commun* 2016; **7**: 12180 [PMID: 27412556 DOI: 10.1038/ncomms12180]

84 **Sozen E**, Demirel-Yalciner T, Sari D, Avcilar C, Samanci TF, Ozer NK. Deficiency of SREBP1c modulates autophagy mediated lipid droplet

catabolism during oleic acid induced steatosis. *Metabol Open* 2021; **12**: 100138 [PMID: 34704008 DOI: 10.1016/j.metop.2021.100138]

85 **Doll S**, Proneth B, Tyurina YY, Panzilius E, Kobayashi S, Ingold I, Irmler M, Beckers J, Aichler M, Walch A, Prokisch H, Trümbach D, Mao G, Qu F, Bayir H, Füllekrug J, Scheel CH, Wurst W, Schick JA, Kagan VE, Angeli JP, Conrad M. ACSL4 dictates ferroptosis sensitivity by shaping cellular lipid composition. *Nat Chem Biol* 2017; **13**: 91-98 [PMID: 27842070 DOI: 10.1038/nchembio.2239]

86 **Duan J**, Wang Z, Duan R, Yang C, Zhao R, Feng Q, Qin Y, Jiang J, Gu S, Lv K, Zhang L, He B, Birnbaumer L, Yang S, Chen Z, Yang Y. Therapeutic targeting of hepatic ACSL4 ameliorates NASH in mice. *Hepatology* 2022; **75**: 140-153 [PMID: 34510514 DOI: 10.1002/hep.32148]

87 **Cotter TG**, Rinella M. Nonalcoholic Fatty Liver Disease 2020: The State of the Disease. *Gastroenterology* 2020; **158**: 1851-1864 [PMID: 32061595 DOI: 10.1053/j.gastro.2020.01.052]

88 **Kim SH**, Seo H, Kwon D, Yuk DY, Jung YS. Taurine Ameliorates Tunicamycin-Induced Liver Injury by Disrupting the Vicious Cycle between Oxidative Stress and Endoplasmic Reticulum Stress. *Life (Basel)* 2022; **12** [PMID: 35330105 DOI: 10.3390/life12030354]

Published by **Baishideng Publishing Group Inc**
7041 Koll Center Parkway, Suite 160, Pleasanton, CA 94566, USA
Telephone: +1-925-3991568
E-mail: office@baishideng.com
Help Desk: https://www.f6publishing.com/helpdesk
https://www.wjgnet.com